

# A General Approach to Twin-T Design and Its Application to Hybrid Integrated Linear Active Networks

By G. S. MOSCHYTZ

(Manuscript received January 2, 1970)

*In this paper we approach twin-T design with a view to controlling the sensitivity of the transmission zero with respect to component variations, according to criteria that are of particular interest in the design of hybrid integrated linear active networks. We give design examples and derive conditions that relate null depth and component characteristics with expected zero displacement in the  $s$ -plane.*

## I. INTRODUCTION

In 1934, H. W. Augustadt invented the twin-T network while carrying out investigations for an economical rectifier filter for phonograph amplifiers.<sup>1</sup> The two main fields of application of the twin-T network were introduced in 1938 by H. H. Scott who discussed its uses as a feedback network to obtain highly selective amplifiers and stable oscillators.<sup>2</sup> In the following years the circuit was thoroughly analyzed in the unloaded state<sup>3-6</sup> and, later, in the loaded state when driven from a nonideal voltage source.<sup>7-9</sup> Consideration was also given to the network's selectivity properties and to the effects of loading and network asymmetry.<sup>10-12</sup> In the early 1960s, a somewhat new application was introduced for the twin-T when synthesis methods based on root locus techniques were developed to employ the twin-T as a compensation network in dc servo systems.<sup>13-15</sup> These investigations were limited to the symmetrical twin-T with fixed source and load resistances. They were later expanded to include wide ranges of source and load impedances<sup>16</sup> and to provide prescribed pole-zero locations<sup>17</sup> using parameter plane techniques.

Recently, with the advent of linear integrated circuits, interest in the twin-T network has been revived yet again, this time by network theoreticians attempting to generate, by RC network synthesis tech-

niques, a still wider range of pole-zero configurations than had hitherto been possible.<sup>18-21</sup> At the same time, numerous methods of active RC filter synthesis were developed that rely on the basic frequency characteristics of a twin-T network or modifications thereof, to provide the required filtering properties.<sup>22-30</sup> These methods depend, for their frequency stability on the stability of the twin-T network. To ensure a very high degree of stability the twin-T has been realized by tantalum thin film components and then combined with silicon integrated active circuits to produce hybrid integrated filter networks.<sup>31</sup> In applications of this kind null frequency and null depth tuning procedures become very critical, particularly because thin film resistors can only be adjusted in the increasing direction; furthermore the null characteristics (gain and phase) become more important than in more conventional applications, and adjustments of these characteristics should not only be possible but also simple. It is with respect to these problems that the twin-T network is reexamined once again here.

The requirement that the six components of a twin-T network provide a perfect null, that is, a pair of imaginary zeros, at a particular frequency imposes only two design constraints on the network. A third results from the impedance scaling factor chosen for the network. Thus, three parameters remain to be chosen by whatever criteria seem most important for a given application. Most often circuit simplicity dominates this choice, resulting in the symmetrical twin-T. In other instances, practical considerations requiring that either all the resistors or all the capacitors be equal will determine the choice. In those cases where the network is synthesized to provide other than standard pole-zero locations, no choice exists at all, since all the network parameters are generally accounted for.

In this paper, we select the three unconstrained design parameters in such a way as to control the null characteristics of the twin-T according to criteria of particular importance in the design of linear active networks. In such networks the twin-T is generally part of a positive or negative feedback configuration whose closed loop poles are closely tied to the open loop zeros on the  $j\omega$ -axis. The latter are generated by the transmission null of the twin-T network. The higher the  $Q$  of the network, the closer the tie between the closed loop poles and the open loop zeros and, consequently, the more critical the sensitivity and stability of the twin-T transmission null. To obtain a measure for both, the zero sensitivity functions for the commonly used and for the general twin-T configurations are derived first. By selecting the three design parameters remaining in the sensitivity functions of the general twin-T

appropriately, it is found that a relatively wide range of sensitivity criteria can be met. Some of these are useful in contributing to the overall stability of an active feedback network incorporating a twin-T. Others are of interest in considerations pertaining to useful frequency and null depth tuning strategies in the vicinity of a perfect twin-T null.

To guarantee stability, conditions are also derived here that prevent the twin-T transmission zeros from drifting to the right half  $s$ -plane. This implies a maximum permissible null depth of the twin-T that can be expressed in terms of the twin-T design parameters and the temperature and aging characteristics of its components.

## 11. CIRCUIT ANALYSIS OF THE GENERAL TWIN-T

The voltage transfer function of the general twin-T shown in Fig. 1 is given by the ratio of two third-order polynomials, namely

$$\frac{E_2}{E_1} = T(s) = \frac{N(s)}{D(s)} = \frac{1 + a_1s + a_2s^2 + a_3s^3}{1 + b_1s + b_2s^2 + b_3s^3} \quad (1)$$

where

$$a_1 = R_3(C_1 + C_2), \quad (2a)$$

$$a_2 = R_3(R_1 + R_2)C_1C_2, \quad (2b)$$

$$a_3 = R_1R_2R_3C_1C_2C_3, \quad (2c)$$

$$b_1 = R_3(C_1 + C_2) + R_2C_2 + R_1(C_2 + C_3), \quad (2d)$$

$$b_2 = R_3[R_1C_3(C_1 + C_2) + (R_1 + R_2)C_1C_2] + R_1R_2C_2C_3, \quad (2e)$$

$$b_3 = R_1R_2R_3C_1C_2C_3 = a_3, \quad (2f)$$

and

$$s = \sigma + j\omega.$$

The null, or transmission zero, of the twin-T is defined by the roots

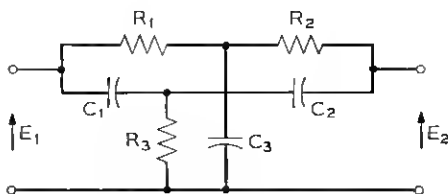


Fig. 1—General twin-T network.

of  $N(s)$  on the imaginary axis. Thus for

$$N(s) \big|_{s=j\omega} = 0 \quad (3)$$

the null frequency or conjugate complex transmission zeros  $z_{1,2} = \pm j\omega_N$  are obtained.

Using the substitutions

$$C_s = \frac{C_1 C_2}{C_1 + C_2}, \quad (4a)$$

$$C_p = C_1 + C_2, \quad (4b)$$

$$R_s = R_1 + R_2, \quad (4c)$$

$$R_p = \frac{R_1 R_2}{R_1 + R_2}, \quad (4d)$$

the following two conditions for the twin-T null frequency result from equation (3)

$$\omega_N^2 = \frac{1}{R_1 R_2 C_s C_3} \quad (5)$$

and

$$\frac{C_3}{R_s} = \frac{C_p}{R_p}. \quad (6)$$

These can be combined as follows

$$\omega_N^2 = \frac{1}{R_1 R_2 C_s C_3} = \frac{1}{R_s R_3 C_1 C_2}. \quad (7)$$

Thus, for a perfect null the transmission zero of each of the two bridged-Ts obtained by disconnecting  $R_s$  and  $C_s$ , respectively, of the twin-T (see Fig. 2) must be equal. This fact has been used to develop a 2-step tuning method for the twin-T.<sup>3,2</sup> Substituting equations (5) and (6) into equation (1) gives the transfer polynomials of the nulled twin-T

$$N(s) = \frac{R_3 C_p}{\omega_N^2} \left( s + \frac{1}{R_s C_p} \right) (s^2 + \omega_N^2) \quad (8)$$

and

$$D(s) = \frac{R_3 C_p}{\omega_N^2} \left( s + \frac{1}{R_s C_p} \right) \left[ s^2 + \left( \omega_N^2 R_1 C_3 + \frac{1}{C_1 R_2} \right) s + \omega_N^2 \right]. \quad (9)$$

The open-circuit impedance matrix of the perfectly nulled twin-T

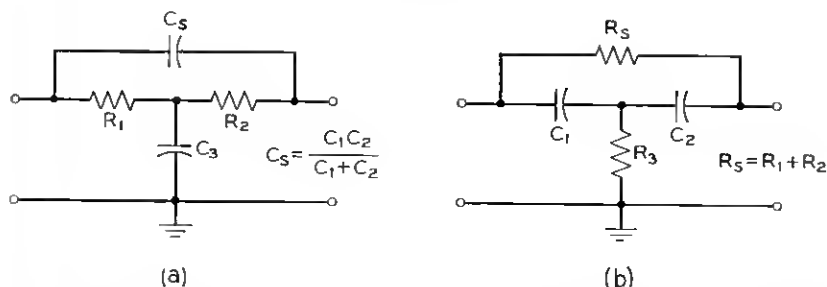


Fig. 2—Bridged-T networks derived from general twin-T shown in Fig. 1, whose natural frequencies coincide with twin-T null frequency. (a)  $R_3$  disconnected; (b)  $C_3$  disconnected.

is given in Appendix A. The voltage transfer function follows from equations (8) and (9), namely

$$T_N(s) = \frac{s^2 + \omega_N^2}{s^2 + \frac{\omega_N}{q_N}s + \omega_N^2} \quad (10)$$

where  $\omega_N$  is given by equation (7),

$$q_N = \frac{\omega_N}{2\sigma_N} = \frac{1}{\omega_N(R_1 C_3 + R_2 C_2)} \quad (11)$$

and

$$2\sigma_N = \omega_N^2 R_1 C_3 + \frac{1}{R_3 C_1} = \frac{1}{R_2 C_2} + \frac{1}{R_3 C_1}. \quad (12)$$

Inspection of equations (8) and (9) shows that the two third-order polynomials of the transfer function of a general twin-T are simplified by one degree due to pole-zero cancellation when the conditions for a perfect null are satisfied. It is shown in Appendix B that even when the twin-T null is *not* perfect (that is, the transmission zeros are not on but only close to the  $j\omega$ -axis), this pole-zero cancellation still takes place, provided that  $R_1 C_1 = R_2 C_2$ .

The most frequently used twin-T is structurally (and electrically) symmetrical (see Appendix A). For this case (see Fig. 3a)  $R_1 = R_2 = R$ ,  $R_3 = R/2$ ,  $C_1 = C_2 = C$ ,  $C_3 = 2C$ , and the coefficients of equation (10) are  $\omega_N = 1/RC$ ,  $2\sigma_N = 4/RC$  and  $q_N = \frac{1}{4}$ . Another commonly used version of the twin-T is the potentially symmetrical configuration (see Appendix A). This is obtained by impedance scaling one-half of the symmetrical twin-T by some factor  $\rho$ . The resulting twin-T elements are

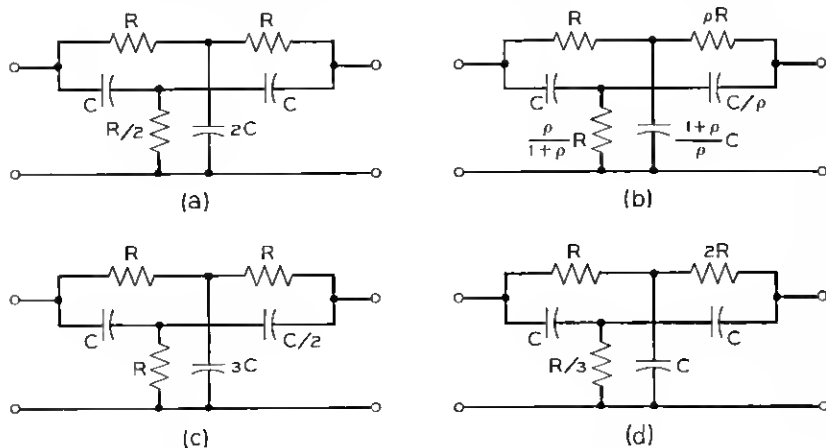


Fig. 3—Frequently used twin-T configurations. (a) Symmetrical; (b) Potentially symmetrical; (c) Equal resistors; (d) Equal capacitors.

(see Fig. 3b)  $R_1 = R$ ,  $R_2 = \rho R$ ,  $R_3 = \rho R/(1 + \rho)$ ,  $C_1 = C$ ,  $C_2 = C/\rho$ , and  $C_3 = (1 + \rho)C/\rho$ . The coefficients of the transfer function [equation (10)] for this case are  $\omega_N = 1/RC$ ,  $2\sigma_N = (2/RC)(1 + \rho)/\rho$  and  $q_N = \frac{1}{2}\rho/(1 + \rho)$ . Notice that for the extreme asymmetrical case for which  $\rho \gg 1$ ,  $q_N$  takes on its maximum value of 0.5.

Sometimes it is useful to make all the resistors of the twin-T equal. This enables one to gang three variable resistors in order to vary the null frequency. The twin-T elements are then (see Fig. 3c)  $R_1 = R_2 = R_3 = R$ ,  $C_1 = C$ ,  $C_2 = C/2$ ,  $C_3 = 3C$ , and the coefficients of the transfer function are the same as those of the symmetrical twin-T. Similarly, if the three capacitors are to be made equal for ganging or other purposes, the twin-T elements are (see Fig. 3d)  $R_1 = R$ ,  $R_2 = 2R$ ,  $R_3 = R/3$ . Here again the coefficients of the transfer function are the same as those of the symmetrical twin-T.

### III. SENSITIVITY OF TWIN-T NULL CHARACTERISTICS TO COMPONENT VARIATIONS

The null or zero sensitivity of the twin-T to variations of any component  $x$  gives a measure for the degree of change of the transmission characteristics in the vicinity of the twin-T null frequency as a result of variations of a component  $x$ . Referring to the complex frequency plane, the zero (or pole) sensitivity gives a measure for the zero (or pole) displacement due to an incremental change in the value of the component

$x$ . It is defined by<sup>33</sup>

$$S'_z = \frac{dz}{dx/x} \quad (13)$$

where  $z$  is the complex null frequency of the network.

The zero displacement  $dz$  in the  $s$ -plane has a real and an imaginary component. It defines a vector or the direction in which a zero (or pole) travels from its initial location with incremental changes of a component  $x$ . Since  $x$  and therefore  $dx/x$  must be real, the zero (pole) sensitivity defines a vector in the same direction as the zero (pole) displacement  $dz$ . Herein lies the importance of knowing the root (that is, pole or zero) sensitivity of a network since it provides insight into the stability of a system with respect to the component  $x$  that is expected to vary the most. It also provides information relevant to network tuning since it relates adjustments of any component  $x$  to its effect on the roots of the transfer function. Conversely, as we shall see later, a network can be designed to provide a prescribed sensitivity between some parameter of the transfer function such as the displacement of a specific transmission zero and the variation of some preselected component  $x$ . The choice of sensitivity may be such as to result in a network that responds to a simplified tuning strategy or whose characteristics may be adjusted in a desirable way by the component  $x$ .

The most important characteristic of the twin-T is its behavior in the region of the frequency null. In the  $s$ -plane this behavior is characterized by the sensitivity of the transmission zero, which is initially located on the imaginary axis for a perfect null. The sensitivities of this zero, that is,  $z = j\omega_N$ , to each of the six components of the general twin-T have therefore been derived in Appendix C and listed in Table I. In doing so it has been found useful to characterize the general twin-T by the following parameters

$$\lambda = \frac{R_1}{R_1 + R_2}, \quad (14)$$

$$\nu = \frac{C_2}{C_1 + C_2}, \quad (15)$$

and

$$\alpha = \frac{\omega_1}{\omega_N} = \left( \frac{R_s C_s}{R_p C_p} \right)^{1/2}. \quad (16)$$

$\lambda$  and  $\nu$  give a measure for the degree of symmetry of the series elements of the twin-T;  $\alpha$  relates the series elements to the shunt elements.

TABLE I—ZERO-SENSITIVITY FUNCTIONS FOR A GENERAL NULLED TWIN-T

$S_{R_1}^{i\omega_N} = \frac{\alpha\omega_N}{2(1+\alpha^2)} \left[ 1 - \lambda - j\left(\frac{1}{\alpha} + \alpha\lambda\right) \right]$	$S_{C_1}^{i\omega_N} = -\frac{\alpha\omega_N}{2(1+\alpha^2)} \left[ 1 - \nu + j\left(\alpha + \frac{\nu}{\alpha}\right) \right]$
$S_{R_2}^{i\omega_N} = \frac{\alpha\omega_N}{2(1+\alpha^2)} \left[ \lambda - j\left(\frac{1}{\alpha} + \alpha(1-\lambda)\right) \right]$	$S_{C_2}^{i\omega_N} = -\frac{\alpha\omega_N}{2(1+\alpha^2)} \left[ \lambda + j\left(\alpha + \frac{(1-\nu)}{\alpha}\right) \right]$
$S_{R_3}^{i\omega_N} = -\frac{\alpha\omega_N}{2(1+\alpha^2)} (1 + j\alpha)$	$S_{C_3}^{i\omega_N} = \frac{\alpha\omega_N}{2(1+\alpha^2)} \left( 1 - \frac{j}{\alpha} \right)$

where:

$$\omega_N^2 = \frac{1}{R_1 R_2 C_1 C_3} = \frac{1}{R_4 R_3 C_1 C_2}$$

$$\omega_1 = \frac{1}{R_3 C_p} = \frac{1}{R_p C_3}$$

$$\alpha = \frac{\omega_1}{\omega_N}; \quad \lambda = \frac{R_1}{R_1 + R_2}; \quad \nu = \frac{C_2}{C_1 + C_2}$$

$$R_s = R_1 + R_2; \quad R_p = \frac{R_1 R_2}{R_1 + R_2}$$

$$C_s = \frac{C_1 C_2}{C_1 + C_2}; \quad C_p = C_1 + C_2$$



A useful check for the validity of the expressions in Table I is that they must satisfy the following condition for the root sensitivity of a passive RC network if the relative resistor and capacitor changes are assumed to track<sup>33</sup>

$$\sum S_{R_i}^z = \sum S_{C_i}^z = -z. \quad (17)$$

Let us now consider the zero sensitivity of the commonly used twin-T configurations shown in Fig. 3.

### 3.1 Symmetrical Twin-T

This case is characterized by the parameters  $\omega_N = 1/RC$ ,  $\alpha = 1$ , and  $\lambda = \nu = 0.5$ . The resulting zero sensitivity functions are listed in Table II, Part 1 and the corresponding zero displacements in the complex frequency plane are shown graphically in Fig. 4a\*. This diagram also demonstrates the realization of the condition for passive RC networks given by equation (17). Therefore, by assuming tracking and equal but opposite temperature coefficients of the resistors and capacitors, temperature drift of the null frequency can theoretically be eliminated completely. If tracking of like component variations does not occur, the drift displacement due to the symmetrical elements  $R_1$  and  $R_2$  and of  $C_1$  and  $C_2$  are identical. The displacements due to the shunt elements  $R_3$  and  $C_3$  have approximately the same value but follow a somewhat less steep slope. Thus if the twin-T is being used in a feedback network to generate conjugate complex poles in the left half plane close to the  $j\omega$ -axis, the stability of the network will be more sensitive to drift in the shunt elements than to drift of those in series.

### 3.2 Potentially Symmetrical Twin-T

This case is characterized by the network parameters  $\omega_N = 1/RC$ ,  $\alpha = 1$ , and  $\lambda = \nu = 1/(1 + \rho)$ . The resulting zero-sensitivity functions are listed in Table II, Part 2. Since they depend on the symmetry coefficient  $\rho$ , some control on the sensitivity can be expected by this coefficient. Table II, Parts 2a and 2b list the sensitivity functions for the two extremes, that is, when  $\rho$  is much larger and much smaller than unity, respectively. The corresponding zero displacements are shown in Fig. 4b. These two complementary cases can be thought of as having evolved from the symmetrical case (Fig. 4a) by spreading out the displacement

\* As pointed out earlier, the root sensitivity function given by equation (13) defines a differential vector in the complex  $s$ -plane. It can be shown that this vector lies on the branch of the root locus with respect to a component  $z$  that starts at  $z$  or, in other words, that the root displacement  $\Delta z$  and the root sensitivity have the same argument.

TABLE II—ZERO-SENSITIVITY FUNCTIONS FOR COMMONLY USED TWIN-T CONFIGURATIONS

1. Symmetrical Twin-T	
$(R_1 = R_2 = 2R_3 = R; C_1 = C_2 = C_3/2 = C): \quad \omega_N = \frac{1}{RC}; \quad q_N = \frac{1}{4}; \quad \alpha = 1; \quad \lambda = \nu = \frac{1}{2}; \quad \gamma = \frac{1}{4}$	
$S_{R_3}^{j\omega_N} = S_{R_3}^{j\omega_N} = \frac{\omega_N}{4} \left( \frac{1}{2} - \frac{3}{2}j \right) = 0.395 \omega_N / -71^\circ 30'$	$S_{C_1}^{j\omega_N} = S_{C_1}^{j\omega_N} = -\frac{\omega_N}{4} \left( \frac{1}{2} + \frac{3}{2}j \right) = -0.395 / 71^\circ 30'$
$S_{R_3}^{j\omega_N} = -\frac{\omega_N}{4} (1 + j) = -0.354 / 45^\circ$	$S_{C_1}^{j\omega_N} = \frac{\omega_N}{4} (1 - j) = 0.354 / -45^\circ$
2. Potentially Symmetrical Twin-T	
$\left[ R_1 = R_2/\rho = R_3(1 + \rho)/\rho = R \right]; \quad \omega_N = \frac{1}{RC}; \quad q_N = \frac{1}{2} \left( \frac{\rho}{1 + \rho} \right); \quad \alpha = 1; \quad \lambda = \nu = \frac{1}{1 + \rho}; \quad \gamma = \frac{\rho}{(1 + \rho)^2}$ $C_1 = \rho C_2 = C_3\rho/(1 + \rho) = C$	
$S_{R_3}^{j\omega_N} = \frac{\omega_N}{4} \left( \frac{\rho}{1 + \rho} - j \frac{2 + \rho}{1 + \rho} \right)$	$S_{C_1}^{j\omega_N} = -\frac{\omega_N}{4} \left( \frac{\rho}{1 + \rho} + j \frac{2 + \rho}{1 + \rho} \right)$
$S_{R_3}^{j\omega_N} = \frac{\omega_N}{4} \left( \frac{1}{1 + \rho} - j \frac{1 + 2\rho}{1 + \rho} \right)$	$S_{C_1}^{j\omega_N} = -\frac{\omega_N}{4} \left( \frac{1}{1 + \rho} + j \frac{1 + 2\rho}{1 + \rho} \right)$
$S_{R_3}^{j\omega_N} = -\frac{\omega_N}{4} (1 + j)$	$S_{C_1}^{j\omega_N} = \frac{\omega_N}{4} (1 - j)$

TABLE II—Cont'd

2A. Potentially Symmetrical Twin-T    ( $s \gg 1$ ): ( $\rho \gg 1$ ): $q_N \rightarrow \frac{1}{2}$ : $\alpha = 1$ ; $\lambda = \nu \rightarrow 0$ ; $\gamma \rightarrow 0$	
$S_{R_1}^{i\omega_N} \approx \frac{\omega_N}{4} (1 - j) = 0.354 \omega_N / \underline{-45^\circ}$	$S_{C_1}^{i\omega_N} \approx -\frac{\omega_N}{4} (1 + j) = -0.354 / \underline{45^\circ}$
$S_{R_2}^{i\omega_N} \approx -j \frac{\omega_N}{2} = 0.5 \omega_N / \underline{-90^\circ}$	$S_{C_2}^{i\omega_N} \approx -j \frac{\omega_N}{2} = 0.5 \omega_N / \underline{-90^\circ}$
$S_{R_3}^{i\omega_N} = -\frac{\omega_N}{4} (1 + j) = -0.354 / \underline{45^\circ}$	$S_{C_3}^{i\omega_N} = \frac{\omega_N}{4} (1 - j) = 0.354 / \underline{-45^\circ}$
2B. Potentially Symmetrical Twin-T    ( $s \ll 1$ ): ( $\rho \ll 1$ ): $q_n \rightarrow 0$ ; $\alpha = 1$ ; $\lambda = \nu \rightarrow 1$ ; $\gamma \rightarrow 0$	
$S_{R_1}^{i\omega_N} \approx -j \frac{\omega_N}{2} = 0.5 \omega_N / \underline{-90^\circ}$	$S_{C_1}^{i\omega_N} \approx -j \frac{\omega_N}{2} = 0.5 \omega_N / \underline{-90^\circ}$
$S_{R_2}^{i\omega_N} \approx \frac{\omega_N}{4} (1 - j) = 0.354 / \underline{-45^\circ}$	$S_{C_2}^{i\omega_N} \approx -\frac{\omega_N}{4} (1 + j) = -0.354 / \underline{45^\circ}$
$S_{R_3}^{i\omega_N} = -\frac{\omega_N}{4} (1 + j) = -0.354 / \underline{45^\circ}$	$S_{C_3}^{i\omega_N} = \frac{\omega_N}{4} (1 - j) = 0.354 / \underline{-45^\circ}$

TABLE II--Cont'd

## 3. Twin-T with Equal Resistors

$$(R_1 = R_2 = R_3 = R; C_1 = 2C_2 = C_3/3 = C): \quad \omega_N = \frac{1}{RC}; \quad q_N = \frac{1}{4}; \quad \alpha = \frac{2}{3}; \quad \lambda = \frac{1}{2}; \quad \nu = \frac{1}{3}; \quad \gamma = \frac{1}{9}$$

$$S_{R_1}^{i\omega_N} = S_{R_2}^{i\omega_N} = \frac{\omega_N}{13} (1.5 - 5.5j) = 0.44 \omega_N / \underline{-75^\circ}$$

$$S_{R_3}^{i\omega_N} = -\frac{\omega_N}{13} (3 + 2j) = -0.278 \omega_N / \underline{34^\circ}$$

$$S_{C_2}^{i\omega_N} = -\frac{\omega_N}{13} (1 + 5j) = -0.392 \omega_N / \underline{79^\circ}$$

$$S_{C_3}^{i\omega_N} = \frac{\omega_N}{13} (3 - 4.5j) = 0.416 \omega_N / \underline{-56^\circ}$$

## 4. Twin-T with Equal Capacitors

$$(R_1 = R_2/2 = 3R_3 = R; C_1 = C_2 = C_3 = C): \quad \omega_N = \frac{1}{RC}; \quad q_N = \frac{1}{4}; \quad \alpha = \frac{3}{2}; \quad \lambda = \frac{1}{3}; \quad \nu = \frac{1}{2}; \quad \gamma = \frac{1}{2}$$

$$S_{R_1}^{i\omega_N} = \frac{\omega_N}{13} (2 - 3.5j) = 0.276 \omega_N / \underline{-60^\circ}$$

$$S_{R_2}^{i\omega_N} = \frac{\omega_N}{13} (1 - 5j) = 0.392 \omega_N / \underline{-79^\circ}$$

$$S_{C_2}^{i\omega_N} = \frac{\omega_N}{13} (3 - 2j) = 0.278 \omega_N / \underline{-34^\circ}$$

$$S_{R_3}^{i\omega_N} = -\frac{\omega_N}{13} (3 + 4.5j) = -0.416 \omega_N / \underline{56^\circ}$$

vectors corresponding to the series components  $R_1$ ,  $R_2$  and  $C_1$ ,  $C_2$ , respectively, and leaving the vectors corresponding to the shunt components  $R_3$  and  $C_3$  unchanged. The noteworthy feature of these two extreme cases is that they both provide for null frequency adjustment (if only over differentially small frequency ranges) by a single component, namely by  $R_2$  or  $C_2$  when  $\rho \gg 1$  and by  $R_1$  or  $C_1$  when  $\rho \ll 1$ . Of the two cases, the former is preferable since it simultaneously provides higher selectivity than a symmetrical twin-T (that is,  $q_N$  approaches its maximum value). More will be said about zero-sensitivity and its effect on network adjustability in Section IV.

### 3.3 *Twin-T With Equal Resistors*

For this case  $\omega_N = 1/RC$ ,  $\alpha = \frac{2}{3}$ ,  $\lambda = \frac{1}{2}$ , and  $\nu = \frac{1}{3}$ . The corresponding zero-sensitivity functions are given in Table II, Part 3, and the zero displacements are shown graphically in Fig. 4c. Since the series resistors are equal in this case, the corresponding sensitivity functions are also equal. However, the sensitivity function of the shunt resistor is smaller in value and flatter in slope. Therefore, in order to shift the null frequency accurately, a high precision ganged 3-resistor potentiometer must be used whose resistor values track very closely.

### 3.4 *Twin-T With Equal Capacitors*

Here we have the design parameters  $\omega_N = 1/RC$ ,  $\alpha = \frac{2}{3}$ ,  $\lambda = \frac{1}{3}$ , and  $\nu = \frac{1}{2}$ . The corresponding sensitivity functions are listed in Table II, Part 4. Since this case is the dual of the equal-resistor case discussed above, the displacement vectors are negative and conjugate to those of Fig. 4c. Generally high precision ganged resistors are more readily available than capacitors, so that for variable null-frequency tuning purposes this case is less practical than the preceding one.

## IV. NOVEL TWIN-T NETWORKS WITH PRESCRIBED TUNING CHARACTERISTICS

In the preceding section, the null sensitivity of component variations was discussed with respect to the most commonly used twin-T configurations. In this section the expressions for the general nulled twin-T, that is, those satisfying only the null conditions given by equations (5) and (6), are reexamined in relation to the corresponding zero sensitivity functions listed in Table I. In particular we investigate how the remaining twin-T parameters that are not constrained by the two null conditions can be utilized to modify the dependence of the null characteristics to adjustments of certain twin-T components in such a way as to

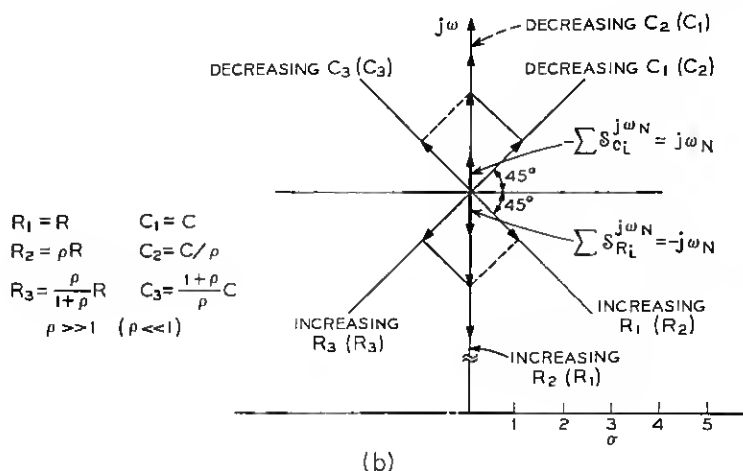
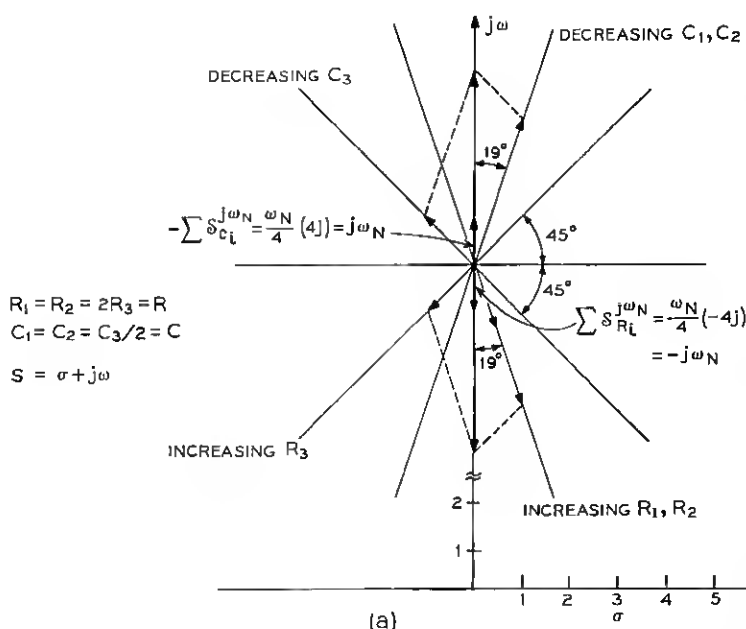
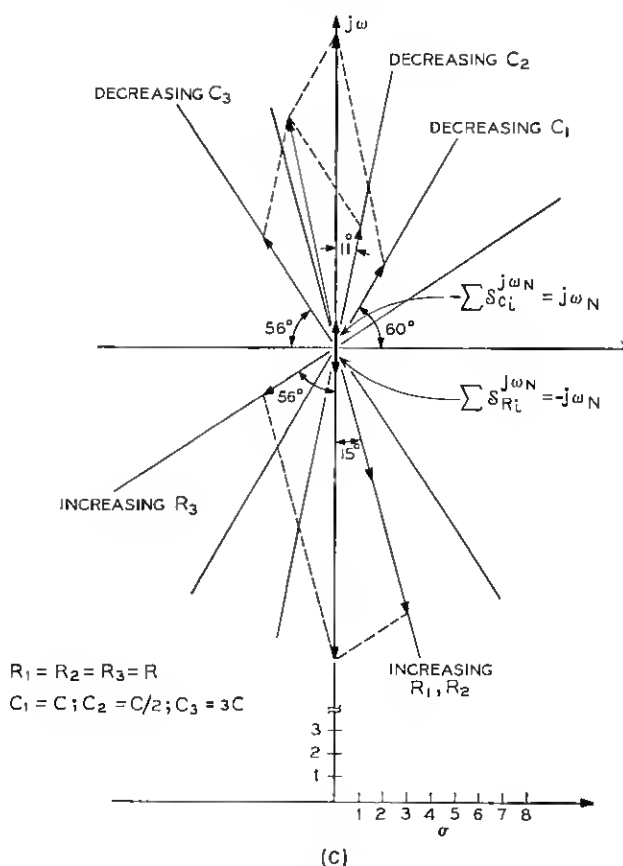


Fig. 4—Zero displacements for frequently used twin-T configurations. (a) Symmetrical; (b) Potentially symmetrical; (c) Equal resistors.



satisfy various tuning strategies that are particularly useful in practical applications.

The dependence of twin-T transmission characteristics in the vicinity of the null frequency on variations of any component  $x$  are essentially determined by the zero sensitivity functions listed in Table I. Design equations for twin-T networks providing a specified dependence of null characteristics on the adjustment of a particular component  $x$  may, therefore, be found by setting corresponding constraints on the zero sensitivity functions and solving the resulting equations for the twin-T components. Instead of designing a twin-T to a specified *dependence of transmission characteristics in the vicinity of the null frequency* to variations of a given component  $x$ , it therefore suffices for us to design a twin-T to a specified *zero sensitivity* with respect to  $x$ .

The expressions listed in Table I show that, after the null frequency  $\omega_N$  has been specified, there are basically three parameters left to determine in order to design a twin-T to a prescribed zero sensitivity. These are the frequency ratio  $\alpha$ , the resistor ratio  $\lambda$ , and the capacitor ratio  $\nu$ . A parameter that sometimes provides clearer physical insight into the design of a twin-T than the frequency ratio  $\alpha$  is the ratio of series to shunt capacitors  $\gamma$ , namely

$$\gamma = \frac{C_2}{C_3} = \nu \frac{C_1}{C_3} \quad (18)$$

The two parameters are related by the expression

$$\alpha = \left[ \frac{\gamma}{\lambda(1 - \lambda)} \right]^{\frac{1}{2}} \quad (19)$$

$\alpha$  has been plotted in Fig. 5 as a function of  $\lambda$  with the parameter  $\gamma$ . The values of  $\gamma$  for the common twin-T configurations are included in Table II. From the defining equations, the limits on the four twin-T parameters are

$$0 < \alpha < \infty, \quad (20a)$$

$$0 < \gamma < \infty, \quad (20b)$$

$$0 < \lambda < 1, \quad (20c)$$

$$0 < \nu < 1. \quad (20d)$$

A fundamental characteristic of the twin-T is its ability to reject a narrow frequency band centered at the null frequency  $f_N$  and to pass, substantially unattenuated, the frequencies on either side of this band. A useful parameter characterizing the selectivity of frequency rejection is the inverse damping factor  $q_N$  [see equation (11)] also known as the pole  $Q$ . Physically  $q_N$  is the ratio of the center frequency  $f_N$  divided by the bandwidth at which 3 dB attenuation occurs\* (see Fig. 6a).

It is important, while examining the effects of the parameters listed in equation (20) on the zero sensitivity of the twin-T to keep an eye on their effect on the twin-T selectivity as expressed by  $q_N$ . Obviously, poor selectivity might be too high a price to pay for any set of controlled sensitivity functions. On the other hand, because the twin-T is a passive RC network, the selectivity factor  $q_N$  only has a narrow range of realiza-

\* This definition is only accurate for unloaded twin-T networks such as those being considered here. For the case of a loaded twin-T with an unsymmetrical frequency response, it has been found more useful to define selectivity as the slope of the phase  $\phi$  at the null frequency, that is, by  $\tau(\omega_N) = d\phi/d\omega|_{\omega=\omega_N}$ .



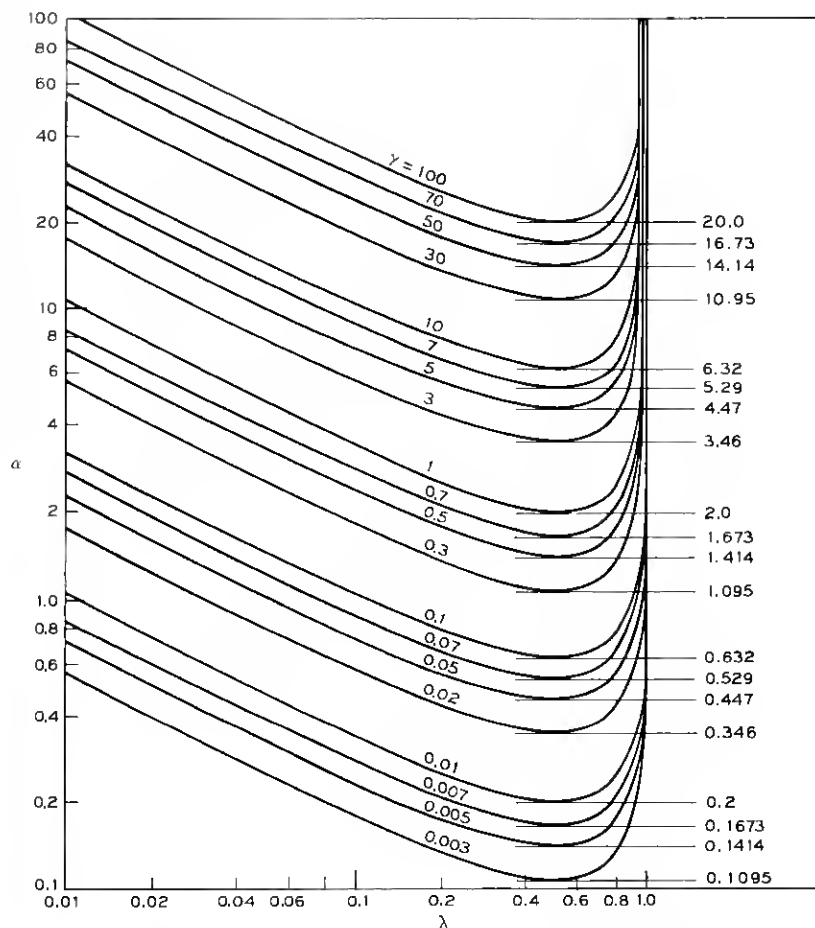


Fig. 5—Frequency ratio  $\alpha$  as a function of  $\lambda$  and parameter  $\gamma$ .

bility as it is, that is,

$$0 < q_N < 0.5 \quad (21)$$

whereby the value 0.25 is realized the most frequently, namely with the symmetrical as well as with the equal resistor or equal capacitor twin-T configurations. However even within the limited range given by equation (21), the difference in actual frequency selectivity can be quite significant. This is illustrated in Fig. 6b where twin-T frequency

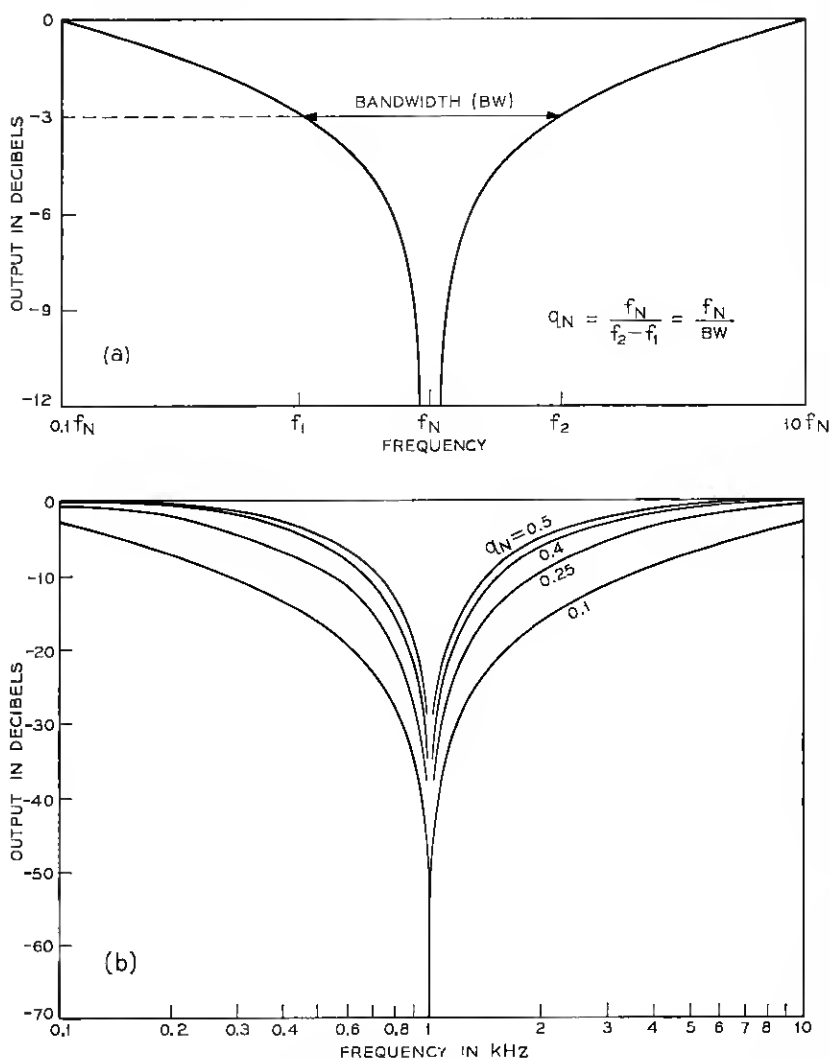


Fig. 6—Twin-T selectivity. (a) Definition of  $q_N$ ; (b) Frequency response for various  $q_N$ -values.

response curves have been plotted as a function of the parameter  $q_N$ .

Expressing  $q_N$  by the same parameters as are used for the zero sensitivity functions in Table I we have

$$q_N = \frac{\alpha(1-\nu)(1-\lambda)}{\alpha^2(1-\lambda) + (1-\nu)} = \frac{(1-\nu)[\gamma\lambda(1-\lambda)]^{\frac{1}{2}}}{\gamma + \lambda(1-\nu)}. \quad (22)$$

With equation (22) we can easily observe the effects on selectivity that any sensitivity constraints on the parameters  $\lambda$ ,  $\nu$ ,  $\alpha$  or  $\gamma$  may have.

After these preliminary remarks, let us now consider in what ways and by which criteria it would be useful in practice to control the zero sensitivity functions given in Table I. Due to the RC self-duality of the twin-T,<sup>34</sup> we need only consider either the resistor or the capacitor functions. Since both discrete and (thin film) integrated RC networks are generally tuned by variable or anodizable *resistors*, the zero sensitivity functions with respect to these will be examined.

#### 4.1 Frequency Tuning by One Component

By making the real part of any one of the three sensitivity functions go to zero, it is possible to shift the null frequency accurately over a limited frequency range by varying only the one corresponding resistor rather than two as would be necessary in general.

##### 4.1.1 Frequency Tuning with $R_1$

Here we require that

$$\operatorname{Re} s_{R_1}^{i\omega_N} \rightarrow 0. \quad (23)$$

By inspection of Table I this condition is fulfilled if  $\lambda \rightarrow 1$ , or  $R_1 \gg R_2$ . Then

$$s_{R_1}^{i\omega_N} \approx -j \frac{\omega_N}{2}, \quad (24a)$$

$$s_{R_1}^{i\omega_N} \approx \frac{\alpha\omega_N}{2(1+\alpha^2)} \left(1 - \frac{j}{\alpha}\right), \quad (24b)$$

$$s_{R_1}^{i\omega_N} = \frac{\alpha\omega_N}{2(1+\alpha^2)} (1 + j\alpha). \quad (24c)$$

Equation (24c) remains the same as for the general case, which is independent of  $\lambda$ . However, from equation (22) we find that

$$q_N|_{\lambda \rightarrow 1} \rightarrow 0. \quad (25)$$

Therefore, condition (23) can only be realized at the expense of selectivity. Incidentally, the potentially symmetrical twin-T for which  $\rho \ll 1$  (see Table II, Part 2b) is a special case of the one treated here, namely, that for which  $\alpha = 1$ .

##### 4.1.2 Frequency Tuning with $R_2$

We require that

$$\operatorname{Re} s_{R_2}^{i\omega_N} \rightarrow 0. \quad (26)$$

This condition can be approached if  $\lambda \rightarrow 0$ , or  $R_2 \gg R_1$ . We then obtain:

$$S_{R_1}^{i\omega_N} \approx \frac{\alpha\omega_N}{2(1+\alpha^2)} \left(1 - \frac{j}{\alpha}\right), \quad (27a)$$

$$S_{R_2}^{i\omega_N} \approx -\frac{j\omega_N}{2}, \quad (27b)$$

$$S_{R_2}^{i\omega_N} = -\frac{\alpha\omega_N}{2(1+\alpha^2)} (1 + j\alpha). \quad (27c)$$

Aside from interchanging the sensitivities with respect to  $R_1$  and  $R_2$ , these expressions are the same as the preceding ones (equations 24a, b, and c). However, there is one important difference, namely in the selectivity which may now actually be larger than the "symmetrical" value of 0.25. From equation (22) we have

$$q_N|_{\lambda=0} = \frac{\alpha(1-\nu)}{\alpha^2 + 1 - \nu}. \quad (28)$$

Depending on the choice of  $\alpha$  and  $\nu$ ,  $q_N$  can be made to approach its maximum value of 0.5. Here again the potentially symmetrical configuration for which  $\rho \gg 1$  is a special case, namely, that for which  $\alpha = 1$  and  $\nu$  approaches zero in the same manner as  $\lambda$  does. This is one of a variety of possible cases for which equation (28) approaches 0.5. Other combinations of  $\alpha$  and  $\nu$  are best obtained by plotting equation (28) on semilog paper as shown in Fig. 7. By setting the derivative of equation (28) with respect to  $\alpha$  equal to zero one obtains

$$\alpha_{\max} = (1 - \nu)^{\frac{1}{2}} \quad (29)$$

and

$$q_{\max} = \frac{(1 - \nu)^{\frac{1}{2}}}{2}. \quad (30)$$

Expression (30) is also shown in Fig. 7 by the dashed curve. Clearly there is a wide practical range of twin-T networks, with good-to-excellent selectivity, that will satisfy condition (26) and thus provide simple frequency tuning over a restricted frequency range.

One of the disadvantages of the twin-T configurations described here is that  $R_2$ , the frequency tuning resistor, is "floating," that is, it does not have one of its terminals connected to ground. Thus if it should be desired to switch various values of  $R_2$  in order to filter or to generate different discrete frequencies, hard-contact switches would generally be

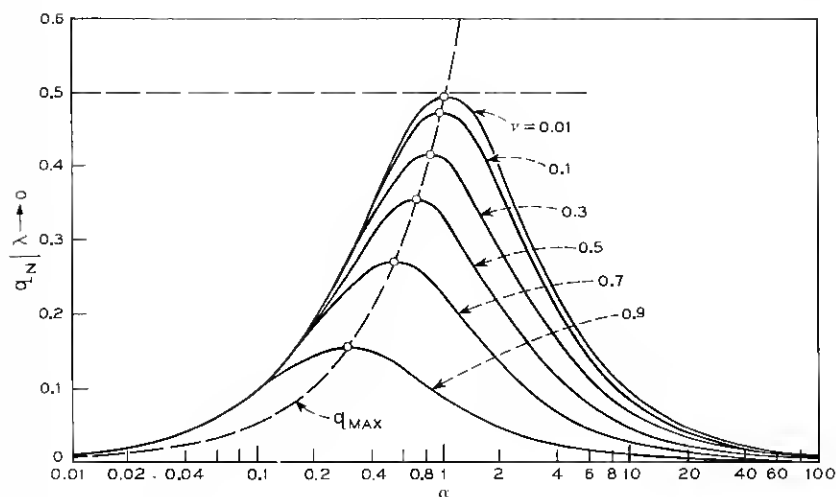


Fig. 7—Selectivity factor  $q_N$  as function of  $\alpha$  and parameter  $\gamma$ , for special case that  $\lambda \rightarrow 0$ .

necessary since rapid semiconductor switching circuits are difficult to design in the floating mode, especially if transformers are to be avoided. For this reason the next case is of particular interest.

#### 4.1.3 Frequency Tuning with $R_3$

The required condition here is that

$$\operatorname{Re} S_{R_1}^{j\omega N} \rightarrow 0. \quad (31)$$

Inspection of Table I shows that this condition cannot be realized under any circumstances. However, the following equivalent condition can be realized

$$\operatorname{Re} S_{R_1}^{j\omega N} \ll I_m S_{R_1}^{j\omega N} \quad (32)$$

if  $\alpha \gg 1$ . Referring to Fig. 5, it is clear that this condition can be obtained in two ways, namely either by letting  $\lambda$  approach zero or unity with a medium value for  $\gamma$  or simply by letting  $\gamma$  become very large. However, by inspection of equation (22), both methods result in low  $q_N$  values. Thus, although the tuning resistor has one terminal grounded which does have certain advantages in terms of circuit implementation, these may be offset by the low selectivity obtainable.

## 4.2 Null-Depth Tuning by One Component

In some applications it may be desirable to make adjustments in the null depth of a twin-T after it has been initially tuned for a perfect null. This can be achieved with a single component (for example, resistor) if the imaginary part of the sensitivity function with respect to that component can be made equal to zero. By considering the general sensitivity functions given in Table I and again restricting ourselves to variable resistors for practical reasons (and because of RC-duality of the twin-T), we obtain the following three cases:

### 4.2.1 Null-Depth Tuning with $R_1$

Here we require that

$$I_{\pi} s_{R_1}^{i\omega_N} \rightarrow 0. \quad (33)$$

The minimum of the imaginary part of  $s_{R_1}^{i\omega_N}$  occurs when  $\lambda = 1/\alpha^2$  in which case the sensitivity functions become

$$s_{R_1}^{i\omega_N} = \frac{\alpha\omega_N}{2(1+\alpha^2)} \left( 1 - \frac{1}{\alpha^2} - j\frac{2}{\alpha} \right) \Big|_{\alpha \gg 1} \approx \frac{\omega_N}{2\alpha}, \quad (34a)$$

$$s_{R_2}^{i\omega_N} = \frac{\alpha\omega_N}{2(1+\alpha^2)} \left( \frac{1}{\alpha^2} - j\alpha \right) \Big|_{\alpha \gg 1} \approx -j\frac{\omega_N}{2}, \quad (34b)$$

$$s_{R_3}^{i\omega_N} = -\frac{\alpha\omega_N}{2(1+\alpha^2)} (1 + j\alpha) \Big|_{\alpha \gg 1} \approx -j\frac{\omega_N}{2}. \quad (34c)$$

As shown in the above expressions, condition (33) is realized by (34a) if  $\alpha \gg 1$ . Furthermore, the other two sensitivity functions turn out to be orthogonal to equation (34a) enabling independent null-frequency and null-depth control by two individual resistors (for example,  $R_1$  and  $R_2$  or  $R_1$  and  $R_3$ ).

It will be remembered that any sensitivity functions requiring large values of  $\alpha$  were dismissed as impractical in the cases presented in Sections 4.1.1 to 4.1.3 due to the resulting decrease in selectivity. This was quite realistic since at least the case in Section 4.1.2 could be realized accurately while maintaining a free choice in the selectivity constant  $q_N$ . We will see in this section that no such freedom exists in any of the cases discussed and that any configuration allowing null-depth tuning by one component invariably results in selectivity deterioration. Practical implementation will therefore require a compromise between the realization of any one of the sensitivity functions and selectivity. However, as will be seen, not all the cases discussed here are equally disadvantageous with respect to this compromise.

Substituting  $\lambda = 1/\alpha^2$  into equation (22), we obtain

$$q_N = \frac{(\alpha^2 - 1)(1 - \nu)}{\alpha(\alpha^2 - \nu)}. \quad (35)$$

To obtain as large a value as possible for  $q_N$ , we let  $\nu \rightarrow 0$  in which case  $q_N \approx 1/\alpha$ . Thus the more accurately we wish to realize expression (34a), the smaller the selectivity will be.

#### 4.2.2 Null-Depth Tuning with $R_2$

The requirement here means that

$$I_m S_{R_2}^{i\omega_N} \rightarrow 0. \quad (36)$$

This would be accurately realizable if we could let

$$\lambda = 1 + \frac{1}{\alpha^2}. \quad (37)$$

Due to the restriction given by inequality (20c), this is not possible. Instead, equation (37) can be approached approximately by letting:

$$\lambda \rightarrow 1 \quad (38a)$$

and

$$\alpha \gg 1. \quad (38b)$$

By inspection of equation (19) and Fig. 5, inequality (38b) follows directly from condition (38a). More specifically, the imaginary part of  $S_{R_2}^{i\omega_N}$  has a minimum when

$$\lambda = 1 - \frac{1}{\alpha^2} \quad (39)$$

which is of course realizable. With equation (39), the sensitivity functions are then

$$S_{R_1}^{i\omega_N} = \frac{\alpha\omega_N}{2(1 + \alpha^2)} \left( \frac{1}{\alpha^2} - j\alpha \right) \Big|_{\alpha \gg 1} \approx -j \frac{\omega_N}{2}, \quad (40a)$$

$$S_{R_2}^{i\omega_N} = \frac{\alpha\omega_N}{2(1 + \alpha^2)} \left( 1 - \frac{1}{\alpha^2} + j \frac{2}{\alpha} \right) \Big|_{\alpha \gg 1} \approx \frac{\omega_N}{2\alpha}, \quad (40b)$$

$$S_{R_3}^{i\omega_N} = -\frac{\alpha\omega_N}{2(1 + \alpha^2)} (1 + j\alpha) \Big|_{\alpha \gg 1} \approx -j \frac{\omega_N}{2}. \quad (40c)$$

Thus equation (40b) provides the desired sensitivity function and also, as in the preceding case, the other two functions are orthogonal to it

allowing for independent frequency and null depth tuning with two individual resistors.

Substituting equation (39) into equation (22), the selectivity function becomes

$$q_N = \frac{1 - \nu}{\alpha(2 - \nu)} \quad (41)$$

which is largest with respect to  $\nu$  when  $\nu \rightarrow 0$ . Then  $q_N \approx 1/2\alpha$  which, as in the previous case, is all the smaller the more accurately the desired sensitivity function (40b) is to be realized. However, the preceding case (namely, that in Section 4.2.1) is preferable if it is simply a question of finding a component with which to adjust null depth, since for a given value of  $\alpha$  the selectivity coefficient is twice as large as here.

#### 4.2.3 Null-Depth Tuning with $R_3$

Here we require that

$$I_m S_{R_3}^{i\omega_N} \rightarrow 0. \quad (42)$$

From Table I it is evident that to satisfy this condition  $\alpha \rightarrow 0$ . From Fig. 5 we see that  $\alpha$  has a minimum when  $\lambda = 0.5$ . Furthermore, since  $\alpha$  is proportional to  $\gamma$ , we can select  $\gamma \ll 1$  in order for  $\alpha$  to approach zero. From equation (22) we obtain the selectivity coefficient

$$q_N = \frac{\alpha(1 - \nu)}{\alpha^2 + 2(1 - \nu)} \quad (43)$$

which is maximum with respect to  $\nu$  when  $\nu \rightarrow 0$ . Therefore from equation (43) we obtain  $q_N \approx \alpha/2$ . The condition for  $\alpha$ , in this case, is the inverse of that for the two preceding cases. Taking this into consideration while comparing the corresponding selectivity coefficients shows the case in Section 4.2.1 to have the highest selectivity. It, like that in 4.2.2, has the added advantage of orthogonal sensitivity functions providing for both the desired null-depth tuning as well as frequency tuning by single components in the vicinity of the null frequency. On the other hand, if a variable component with one terminal grounded is preferred for the reasons given in Section 4.1.2, then the case in Section 4.2.3 may be used, provided the selectivity, which is smaller by a factor of two, is still acceptable.

#### 4.3 Orthogonal Tuning With Two Components

Orthogonality between two zero sensitivity functions simplifies null adjustments in the vicinity of a perfect null, particularly if the two



functions are parallel with the real and imaginary axes. Some of the configurations described in the previous sections provided the latter type of orthogonality, but only at the cost of selectivity. General orthogonality, which is discussed here, may be of interest for a variety of reasons, for example, the 90 degree phase reference required for tuning purposes may be easier to generate than any other arbitrary phase reference.

Two vectors  $\mathbf{q} = u + jv$  and  $\mathbf{p} = w + jz$  are orthogonal if

$$uw + vz = 0. \quad (44)$$

Thus, to obtain orthogonality between pairs of the functions listed in Table I, we must investigate if they can be made to satisfy this condition.

#### 4.3.1 Orthogonal Tuning Between $R_1$ and $R_2$

This requires that

$$\lambda(1 - \lambda) + \left(\frac{1}{\alpha} + \alpha\lambda\right)\left[\frac{1}{\alpha} + \alpha(1 - \lambda)\right] = 0. \quad (45)$$

Solving for the roots of this equation one obtains  $\alpha_{1,2} = \pm j$  which is not physically realizable.

#### 4.3.2 Orthogonal Tuning Between $R_1$ and $R_3$

To satisfy the condition for orthogonality here, we require that

$$-(1 - \lambda) + \alpha\left(\frac{1}{\alpha} + \alpha\lambda\right) = 0. \quad (46)$$

Solving equation (46) for  $\alpha$  results in the same nonrealizable roots as were obtained in Section 4.3.1. However, one additional solution exists here, namely  $\lambda = 0$ . This condition can only be approximated [see inequality (20c)] and has been dealt with in Sections 4.1.2 and 4.2.1 where, as expected,  $S_{R_1}^{i\omega_N}$  is orthogonal to  $S_{R_3}^{i\omega_N}$ .

#### 4.3.3 Orthogonal Tuning Between $R_2$ and $R_3$

It is required that

$$-\alpha + \alpha\left[\frac{1}{\alpha} + \alpha(1 - \lambda)\right] = 0 \quad (47)$$

which is satisfied when  $\lambda = 1$ . As in the preceding case, this condition can only be approximated; it has been dealt with in Sections 4.1.1 and 4.2.2.

It is evident from the above that, apart from the cases of orthogonality already discussed in earlier sections, the condition for general orthog-

onality given by equation (44) does not produce any new realizable twin-T configurations.

#### 4.4 Design Examples of Twin-T Networks With Controlled Tuning Characteristics

The design equations for twin-T networks with the tuning characteristics described in Sections 4.1 and 4.2 have been compiled in Table III. Results from Section 4.3 have not been included since they did not

TABLE III—TWIN-T DESIGN EQUATIONS FOR CONTROLLED ZERO SENSITIVITY

Design Equations for Controlled Sensitivity and Sensitivity Functions	Design Equations for Maximum Selectivity	Remarks
1A) $\text{Re } S_{R_1}^{i u N} \rightarrow 0: \quad \lambda \rightarrow 1$ $S_{R_1}^{i u N} \approx -j \frac{\omega_N}{2}$ $S_{R_1}^{i u N} \approx \frac{\alpha \omega_N}{2(1 + \alpha^2)} \left(1 - \frac{j}{\alpha}\right)$ $S_{R_1}^{i u N} = -\frac{\alpha \omega_N}{2(1 + \alpha^2)} \left(1 - \frac{j}{\alpha}\right)$	$q_N \Big _{\lambda \rightarrow 0} \approx \frac{\alpha(1 - \lambda)}{\alpha^2(1 - \lambda) + 1}$ $q_{N \max} \Big _{\lambda \rightarrow 0} \approx \frac{\sqrt{1 - \lambda}}{2}$ where: $\alpha = \frac{1}{\sqrt{1 - \lambda}}$	$q_N \ll 0.5$  Orthogonality between $S_{R_1}^{i u N}$ and $S_{R_1}^{i u N}$
1B) $\text{Re } S_{R_1}^{i u N} \rightarrow 0: \quad \lambda \rightarrow 0$ $S_{R_1}^{i u N} \approx \frac{\alpha \omega_N}{2(1 + \alpha^2)} \left(1 - \frac{j}{\alpha}\right)$ $S_{R_1}^{i u N} \approx -\frac{j \omega_N}{2}$ $S_{R_1}^{i u N} = -\frac{\alpha \omega_N}{2(1 + \alpha^2)} (1 + j\alpha)$	$q_N \approx \frac{\alpha(1 - \nu)}{\alpha^2 + 1 - \nu}$ $q_{N \max} \approx \frac{(1 - \nu)^{1/2}}{2}$ where: $\alpha_{\max} = (1 - \nu)^{1/2}$	$0 < q_N < 0.5$  Orthogonality between $S_{R_1}^{i u N}$ and $S_{R_1}^{i u N}$
1C) $\text{Re } S_{R_1}^{i u N} \rightarrow 0: \quad \alpha \gg 1$ $S_{R_1}^{i u N} = \frac{\alpha \omega_N}{2(1 + \alpha^2)} \left[1 - \lambda - j\left(\frac{1}{\alpha} + \alpha\lambda\right)\right]$ $S_{R_1}^{i u N} = \frac{\alpha \omega_N}{2(1 + \alpha^2)} \left[\lambda - j\left(\frac{1}{\alpha} + \alpha(1 - \lambda)\right)\right]$ $S_{R_1}^{i u N} \approx -j \frac{\omega_N}{2}$	$q_N \approx \frac{1 - \nu}{\alpha}$ $q_{N \max} \approx \frac{1}{\alpha}$ for $\nu \rightarrow 0$	$q_N \ll 0.5$  Variable resistor ( $R_3$ ) has one common (that is, grounded) terminal

TABLE III—Cont'd

Design Equations for Controlled Sensitivity and Sensitivity Functions	Design Equations for Maximum Selectivity	Remarks
2A)  Im $s_{R_1}^{j\omega_N} \rightarrow 0$ : $\alpha \gg 1$ $\lambda = \frac{1}{\alpha^2} \ll 1$	$q_N \approx \frac{(\alpha^2 - 1)(1 - \nu)}{\alpha(\alpha^2 - \nu)}$  $q_{N \max} \approx \frac{1}{\alpha}$  for $\nu \rightarrow 0$	$q_N \ll 0.5$  Orthogonality between  $s_{R_1}^{j\omega_N}$ and $s_{R_1}^{j\omega_N} = s_{R_1}^{j\omega_N}$
$s_{R_1}^{j\omega_N} \approx \frac{\omega_N}{2\alpha}$  $s_{R_1}^{j\omega_N} \approx -j \frac{\omega_N}{2}$  $s_{R_1}^{j\omega_N} \approx -j \frac{\omega_N}{2}$		
2B)  Im $s_{R_1}^{j\omega_N} \rightarrow 0$ : $\alpha \gg 1$ $\lambda = \left(1 - \frac{1}{\alpha}\right) \rightarrow 1$	$q_N \approx \frac{1 - \nu}{\alpha(2 - \nu)}$  $q_{N \max} \approx \frac{1}{2\alpha}$  for $\nu \rightarrow 0$	$q_N \ll 0.5$  Orthogonality between  $s_{R_1}^{j\omega_N}$ and $s_{R_1}^{j\omega_N} = s_{R_1}^{j\omega_N}$
$s_{R_1}^{j\omega_N} \approx -j \frac{\omega_N}{2}$  $s_{R_1}^{j\omega_N} \approx \frac{\omega_N}{2\alpha}$  $s_{R_1}^{j\omega_N} \approx -j \frac{\omega_N}{2}$		
2C)  Im $s_{R_1}^{j\omega_N} \rightarrow 0$ : $\alpha \rightarrow 0$ $\lambda = 0.5$	$q_N \approx \frac{\alpha(1 - \nu)}{\alpha^2 + 2(1 - \nu)}$  $q_{N \max} \approx \frac{\alpha}{2}$  for $\nu \rightarrow 0$	$q_N \ll 0.5$  Variable resistor ( $R_3$ ) has one common (that is, grounded) terminal
$s_{R_1}^{j\omega_N} \approx \frac{\omega_N}{2} \left(\frac{\alpha}{2} - j\right)$  $s_{R_1}^{j\omega_N} \approx \frac{\omega_N}{2} \left(\frac{\alpha}{2} - j\right)$  $s_{R_1}^{j\omega_N} \approx -\frac{\alpha\omega_N}{2}$		

produce anything not already obtained in the two previous sections.

Using the design equations listed in Table III, the detailed procedure for the design of two twin-T networks with prescribed tuning characteristics follows.

#### 4.4.1 Twin-T With Null Frequency Tunable by $R_2$

To satisfy condition (26), we find from Table III, Part 1B, that  $\lambda \ll 1$

and therefore select  $\lambda = 0.01$ . Furthermore, assuming that  $q_N = 0.25$ ,  $\omega_N = 2\pi 1$  kHz, and  $R_1 = 1$  K $\Omega$ , we find  $R_2 = 99$  K $\Omega$ . From Fig. 7 we find that the  $q_{\max}$ -curve passes through the value 0.25 when  $\alpha = 0.5$ . However, with  $\lambda = 0.01$ ,  $\gamma$  takes on a simpler value for  $\alpha = 0.55$  (see Fig. 5), namely

$$\gamma = \alpha^2 \lambda (1 - \lambda) = 0.003.$$

Solving equation (28) for  $\nu$  we obtain

$$\nu = 1 - \frac{\alpha^2}{4\alpha - 1} = 0.75$$

and from equation (18)

$$C_1 = \frac{\gamma}{\nu} \cdot C_3 = 0.004 C_3.$$

From equations (5) and (18)

$$C_3 = \frac{1}{\omega_N (\gamma R_1 R_2)^{\frac{1}{2}}} = 0.292 \mu\text{F}$$

and

$$C_1 = \frac{\gamma}{\nu} C_3 = 1.168 \text{ nF}.$$

Finally, with equation (15)

$$C_2 = \frac{\nu}{1 - \nu} C_1 = 3.504 \text{ nF}$$

and, from equation (6)

$$R_3 = \frac{C_3}{C_p} \cdot R_p = 62 \text{ K}.$$

The corresponding sensitivity functions can be calculated directly by substituting the values obtained above into the expressions listed in Table I. Considering only the relative values of the resistor sensitivity functions, one obtains

$$S_{R_1}^{i\omega_N} = \frac{\alpha\omega_N}{2(1 + \alpha^2)} (0.99 - 1.83j),$$

$$S_{R_2}^{i\omega_N} = \frac{\alpha\omega_N}{2(1 + \alpha^2)} (0.01 - 2.365j),$$

$$S_{R_3}^{i\omega_N} = \frac{\alpha\omega_N}{2(1 + \alpha^2)} (1 + 0.55j).$$

The twin-T network resulting from the above calculations, as well as the zero displacement vectors given above, are shown in Fig. 8. In Fig. 9a, measurements of the frequency response of this twin-T are compared with those of a symmetrical twin-T nulled at the same frequency. The initial frequency response of the two ideally nulled networks are identical since both have a selectivity constant  $q_N$  equal to 0.25. On varying  $R_2$ , however, the null depth of the symmetrical network decreases considerably with varying null frequency compared to that of the non-symmetrical configuration. This is also apparent from Fig. 9b, where the percentage frequency shift of the null is shown as a function of the relative resistor change  $R_2$ . Whereas this curve is not appreciably different for the two configurations, the simultaneous variation in null depth is.

#### 4.4.2 Twin-T with Null Depth Tunable by $R_3$

To satisfy condition (42), we find from Table III, Part 2C, that  $\alpha \ll 1$  and select  $\alpha = 0.1$ . Furthermore, with  $\lambda = 0.5$  and letting  $\nu = 0.01$ , for maximum selectivity, we find from equation (22) that  $q_N = 0.048$ .

As in the previous example, we assume that  $\omega_N = 2\pi \cdot 1$  kHz and, because  $\lambda = 0.5$ , we select  $R_1 = R_2 = 10$  K $\Omega$ . From equation (19) we find  $\gamma = 0.0025$  and, in precisely the same way as in the preceding example,  $C_3 = 0.318$   $\mu$ F,  $C_1 = 79.5$  nF,  $C_2 = 0.804$  nF, and  $R_3 = 19.8$  K. The corresponding zero sensitivity functions follow directly from Table I. The relative values of the resistor sensitivity functions are

$$S_{R_1}^{i\omega_N} = \frac{\alpha\omega_N}{2(1 + \alpha^2)} (0.5 - 10.05j),$$

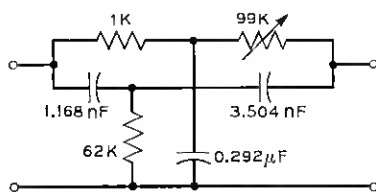
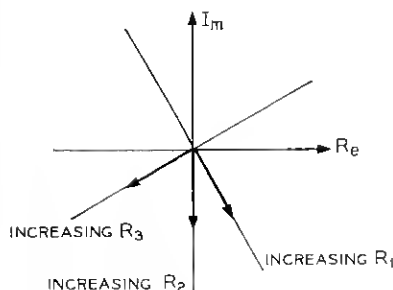


Fig. 8—Zero displacement and twin-T configuration for  $\omega_N = 2\pi \cdot 1$  kHz,  $q_N = 0.25$ ,  $\lambda = 0.01$ ,  $\nu = 0.75$ ,  $\alpha = 0.55$ .

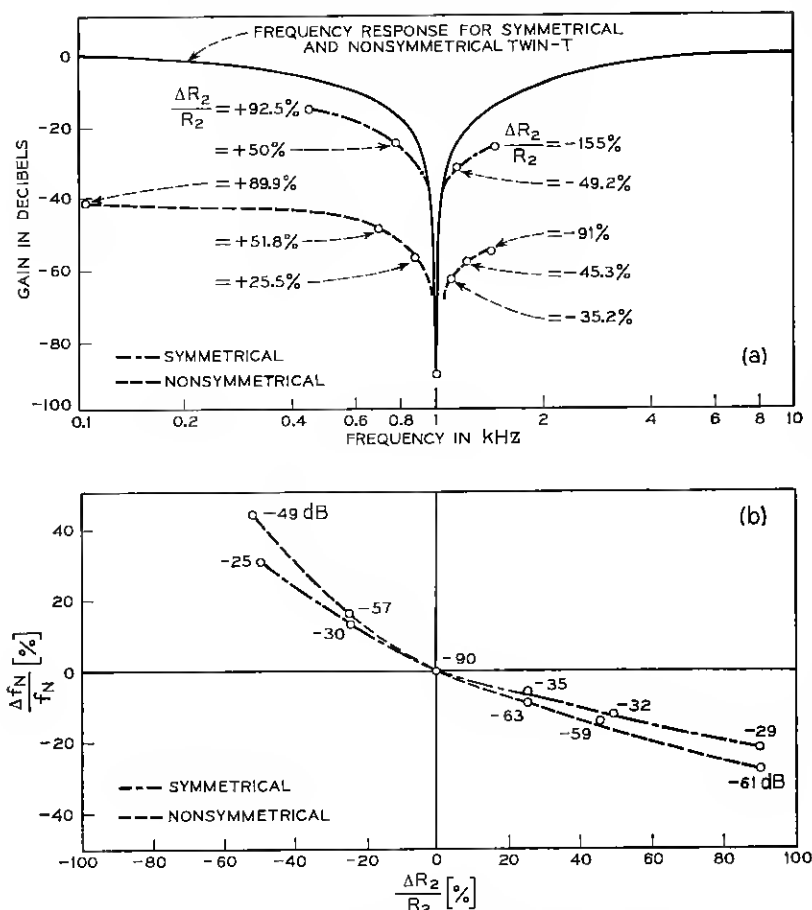


Fig. 9—Comparison of measurements conducted on twin-T shown in Fig. 8 and symmetrical twin-T. (a) Null-frequency shift and null-depth variation with variation of  $R_2$ ; (b) Twin-T null frequency as function of percentage change in  $R_2$ .

$$S_{R_2}^{i\omega_N} = \frac{\alpha\omega_N}{2(1+\alpha^2)} (0.5 - 10.05j),$$

$$S_{R_2}^{i\omega_N} = -\frac{\alpha\omega_N}{2(1+\alpha^2)} (1 + 0.1j),$$

The resulting twin-T network and the zero displacement vectors are shown in Fig. 10. Measurements made on the twin-T are shown in Fig. 11a where they are compared with those of a symmetrical network

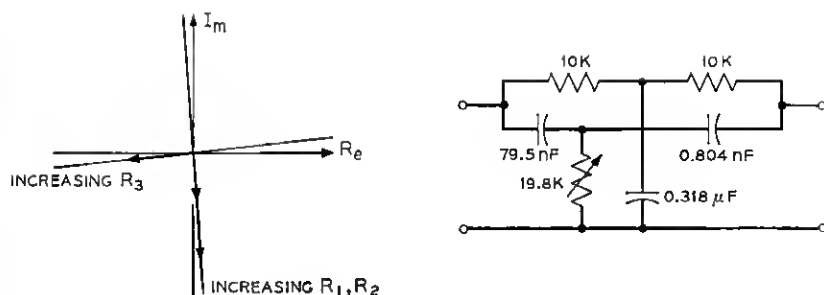


Fig. 10—Zero displacement and twin-T configuration for  $\omega_N = 2\pi \cdot 1$  kHz,  $q_N = 0.048$ ,  $\lambda = 0.5$ ,  $\nu = 0.01$ ,  $\alpha = 0.1$ .

with the same null frequency. The initial frequency response of the two configurations differs here, since the selectivity coefficient of the symmetrical twin-T is 0.25, and that of the other is 0.048. The null depth of the symmetrical twin-T can be decreased by more than 50 dB from an initial 90-dB null with no measurable change in the null frequency. This compares with over 1 percent variation of null frequency for the symmetrical configuration. This is shown again in Fig. 11b where the null depth variation is plotted versus relative change in the resistor  $R_3$ .

#### V. TWIN-T NULL STABILITY USING THIN FILM COMPONENTS

The twin-T is frequently used to provide stable zeros in the design of hybrid integrated linear active networks. If a high degree of stability is required, thin film components must be used for the twin-T network. Just what degree of null stability can be expected with thin film components whose temperature coefficients and aging characteristics are known, follows directly from the sensitivity functions discussed in the previous sections. This is shown in the following.

A displacement  $dz$  in the transmission zero  $z$  of a twin-T network can be expressed in terms of the zero sensitivity defined by equation (13) as follows

$$dz = \sum_{i=1}^3 s_{R_i}^z \frac{dR_i}{R_i} + \sum_{i=1}^3 s_{C_i}^z \frac{dC_i}{C_i}. \quad (48)$$

As shown in Fig. 12, if the twin-T transmission zero is close to the  $j\omega$ -axis it can be considered purely imaginary for purposes of computing sensitivities, thus

$$s_x^z \approx s_x^{j\omega_N}. \quad (49)$$

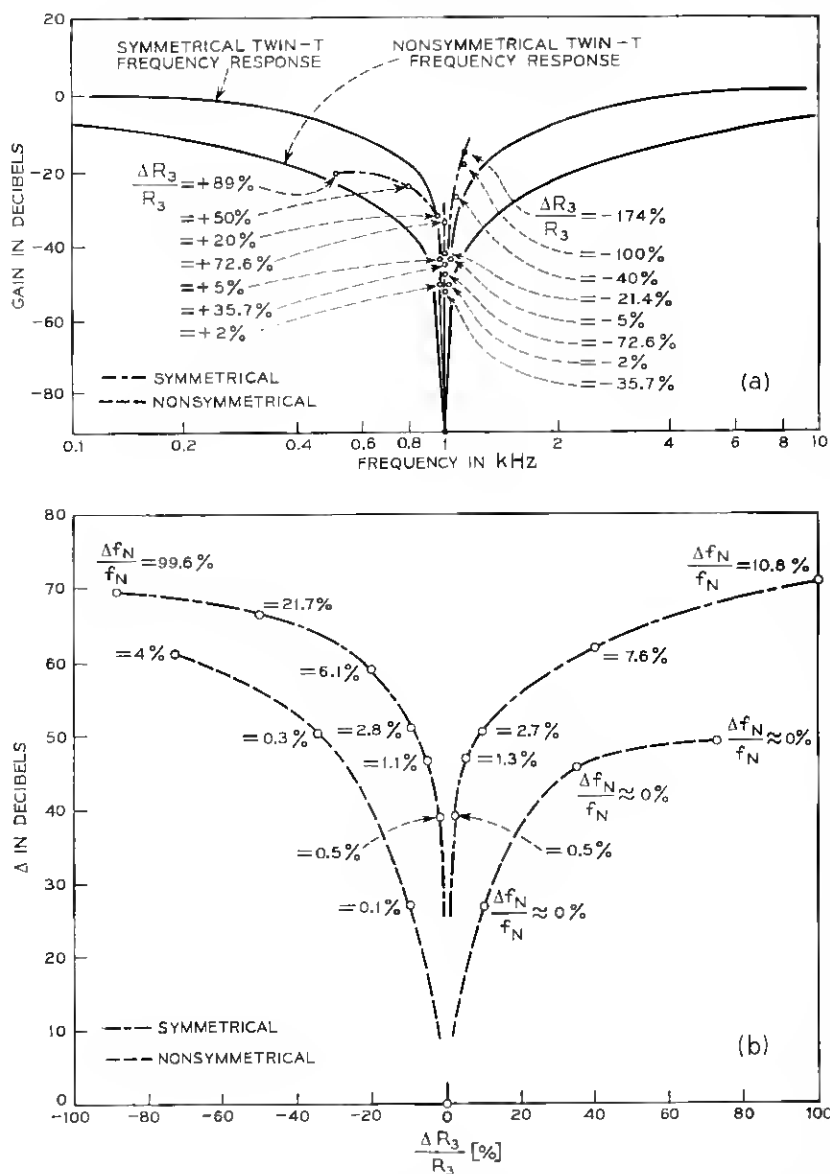


Fig. 11—Comparison of measurements conducted on twin-T shown in Fig. 10 and symmetrical twin-T. (a) Null-frequency shift and null-depth variation with variation of  $R_3$ ; (b) Twin-T null depth as function of percentage change in  $R_3$ .



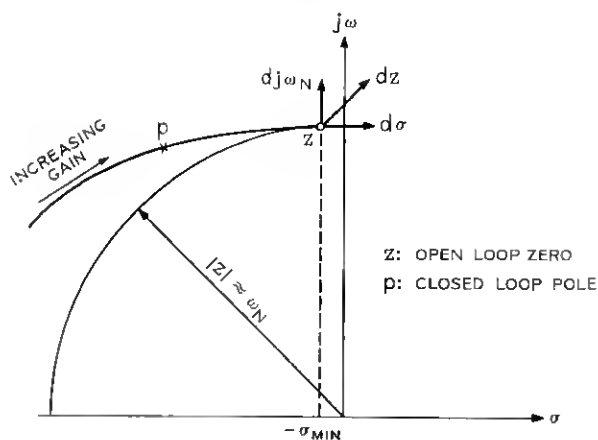


Fig. 12—Typical root locus of feedback network using a twin-T to provide the open loop zeros.

Furthermore, referring again to Fig. 12, the zero displacement is given as

$$dz = d\sigma + dj\omega_N. \quad (50)$$

Equating (48) and (50) and substituting the expressions of Table I in equation (48), it is possible to solve for  $d\sigma$  and  $dj\omega_N$ .

First, however, some characteristics peculiar to thin film integrated circuitry must be considered. Due to the batch processing techniques used, component uniformity can be guaranteed much more accurately than with discrete components. Above all, component variations tend to track very closely on a given glass or ceramic substrate and these variations can be precisely predicted and controlled. These features permit a considerable simplification in the following calculations without any loss in accuracy. Thus, we can write

$$\frac{\Delta R_i}{R_i} = [\delta_r \pm \epsilon_r] \Delta T + \kappa_r = \frac{\Delta R}{R} \quad (51)$$

and

$$\frac{\Delta C_i}{C_i} = [\delta_c \pm \epsilon_c] \Delta T + \kappa_c = \frac{\Delta C}{C}. \quad (52)$$

The temperature coefficients of the resistors and capacitors are  $\delta_r$  and  $\delta_c$ , respectively;  $\epsilon_r$  and  $\epsilon_c$  are the tracking ratios between the three resistors and the three capacitors, respectively;  $\Delta T$  is the temperature

range under consideration; and  $\kappa_r$  and  $\kappa_c$  are the percentage resistor and capacitor aging, respectively. Substituting equations (51) and (52) as well as the expressions in Table I into equation (48), we obtain for the real part of the finite zero displacement  $\Delta z = \Delta\sigma + j\Delta\omega_N$

$$\frac{\Delta\sigma}{\omega_N} = \frac{\alpha}{2(1 + \alpha^2)} [\epsilon_c(1 - \nu) - \epsilon_r(1 - \lambda)] \Delta T. \quad (53)$$

Notice that the zero displacement parallel to the real axis depends only on the *amount of mistracking between components* and not on the absolute drift of the individual components. In other words, if all components of a kind drift by the same percentage, the null depth of a tuned twin-T will not change. This is to be expected since *equal component drift corresponds to a frequency scaling process*.

The imaginary part of the finite zero displacement  $\Delta z$  is obtained in the same way as the real displacement above. Thus

$$\begin{aligned} -\frac{\Delta\omega_N}{\omega_N} &= (\delta_r + \delta_c) \Delta T + \kappa_r + \kappa_c \\ &+ \frac{\epsilon_r \Delta T}{2} \left[ \frac{1 + \alpha^2(2 - \lambda)}{1 + \alpha^2} \right] + \frac{\epsilon_c \Delta T}{2} \left[ \frac{\alpha^2 + 2 - \nu}{1 + \alpha^2} \right]. \end{aligned} \quad (54)$$

Thus, the zero displacement along the  $j\omega$ -axis depends on the actual drift of the individual components. Clearly, if the drift coefficients of the resistors can be made equal but opposite to those of the capacitors, drift along the  $j\omega$ -axis can be practically eliminated.

In various active filter schemes the network poles are tied closely to the transmission zeros generated by a twin-T. Thus, in high  $Q$  networks, uncontrolled drift of the twin-T zero into the right-half  $s$ -plane could pull the poles over with it, causing oscillation. Similarly, drift of the twin-T zero along the  $j\omega$ -axis would cause frequency drift in the active filter.

To prevent oscillation due to drift into the right half plane, the transmission zero of the twin-T must be located left of the  $j\omega$ -axis by some distance  $\sigma_{\min}$  such that, under worst case component drift, it will not travel across the  $j\omega$ -axis. Referring to Fig. 12, this implies that

$$\sigma_{\min} \geq \text{Re}(\Delta z_{\max}) = \Delta\sigma_{\max}. \quad (55)$$

This condition, in turn, implies that the twin-T null depth may not exceed a certain maximum attenuation  $T_{N \max}$  which can now be calculated directly.

It follows from Appendix B that the transfer function of a twin-T

with a nonperfect null can be approximated as follows

$$T_N(s) \approx \frac{s^2 + 2\sigma s + \omega_N^2}{s^2 + \frac{\omega_N}{q_N}s + \omega_N^2}. \quad (56)$$

With equation (55), the maximum null attenuation for left half plane transmission zeros is then

$$T_{N \max} |_{s=j\omega_N} = 2 \frac{q_N}{\omega_N} \sigma_{\min} = 2 \frac{q_N}{\omega_N} \Delta \sigma_{\max}. \quad (57)$$

With equations (22) and (53) this becomes

$$T_{N \max} = \frac{\alpha^2}{1 + \alpha^2} \left( \frac{(1 - \nu)(1 - \lambda)}{\alpha^2(1 - \lambda) + (1 - \nu)} \right) [\epsilon_r(1 - \lambda) + \epsilon_c(1 - \nu)] \Delta T. \quad (58)$$

In active filter applications where the twin-T transmission zero  $z$  represents the open loop zero of the root locus of a pole  $p$  with respect to gain (see Fig. 12), the highest attainable  $Q$  of the network is all the more limited the larger  $\sigma_{\min}$  has to be chosen for stability. In the limit, as the loop gain approaches infinity, the closed loop pole  $p$  coincides with  $z$ . The upper limit on  $Q$  is therefore given by

$$Q_{\max} < \frac{\omega_N}{2\sigma_{\min}} \quad (59)$$

or, with equation (53)

$$Q_{\max} < \frac{(1 + \alpha^2)}{\alpha \Delta T} \left( \frac{1}{\epsilon_r(1 - \lambda) + \epsilon_c(1 - \nu)} \right). \quad (60)$$

Thus, with the type of active network design represented by the root locus in Fig. 12, both network stability and maximum  $Q$  ultimately depend on the stability of the twin-T network.

As an example of the above, we shall consider the stability of a symmetrical twin-T network fabricated with tantalum thin film resistors and capacitors. The required ambient temperature range is assumed to be from 0°C to 60°C. From equation (58) we obtain

$$T_{N \max} \Big|_{\substack{\lambda = \nu = 0.5 \\ \alpha = 1}} = \frac{1}{16} [\epsilon_r + \epsilon_c] \Delta T. \quad (61)$$

Typically, for tantalum thin film resistors and capacitors  $\epsilon_r = \pm 5$  ppm/°C and  $\epsilon_c = \pm 15$  ppm/°C. Therefore  $T_{N \max} = 7.510^{-5} = -83$  dB.

The frequency drift for a symmetrical twin-T results from equation (54) as

$$-\frac{\Delta\omega_N}{\omega_N} = [(\delta_r + \delta_c) + \frac{5}{8}(\epsilon_r + \epsilon_c)] \Delta T' + \kappa_r + \kappa_c. \quad (62)$$

Typically, for tantalum thin film components  $\kappa_r = \kappa_c = 0.1\%$  and for tantalum thin film capacitors  $\delta_c = 200$  ppm/ $^{\circ}\text{C}$ . The TC of tantalum thin film resistors can be controlled by oxygen doping during the sputtering process.<sup>35</sup> It may therefore be of interest to solve equation (62) for the required TCR, that is,  $\delta_r$ , when a maximum acceptable frequency drift is specified. Assuming that  $(\Delta\omega_N/\omega_N)_{\max} \leq 0.5\%$  we obtain  $\delta_r = (-215 \pm 50)$  ppm/ $^{\circ}\text{C}$ .

## VI. CONCLUSIONS

Design equations have been presented that provide twin-T configurations with null characteristics that depend on individual component variations in a predictable and controlled manner. This is achieved by deriving the zero sensitivity functions with respect to each component of the general nulled twin-T. The network parameters required to obtain a twin-T that can be tuned by a desired procedure and the extent to which such a procedure can at all be realized results directly from inspection of the general sensitivity functions.

Special null tuning procedures are considered that are useful in linear active networks incorporating a twin-T in the feedback path. One twin-T configuration permits the null frequency to be shifted over a limited range by the variation of one component only while the null depth remains constant. Another enables the null depth to be varied by one component with negligible variation in the null frequency. The possibility of independent null frequency and null depth tuning by two individual components is also investigated. Orthogonal sensitivity functions that are parallel to the real and imaginary axis are required to do this. It is shown that, apart from the orthogonality that is obtained as a by-product in the first two cases, any other or more general kind of orthogonality in the sensitivity functions cannot be realized. Design examples for the first two cases are given. Measurements conducted on the resulting twin-T configurations are presented and compared with similar measurements made on a conventional, that is, symmetrical, twin-T. This comparison demonstrates the effectiveness of the given design equations.

The stability of the null characteristics of a twin-T with given

component characteristics results directly from the sensitivity functions. Limits on the permissible null depth of a twin-T are derived for the case that left-half plane zeros must be guaranteed under worst case component drift conditions. Similarly, expressions are derived that permit the limits on resistor and capacitor temperature coefficients and aging characteristics to be established in order not to exceed a given maximum frequency drift of the transmission null. A numerical example is given using the characteristics of tantalum thin film resistors and capacitors.

## VII. ACKNOWLEDGMENT

Thanks are due to G. Malek who carried out the twin-T measurements shown in Figs. 9 and 11.

## APPENDIX A

### *Twin-T Impedance Matrix*

In order to calculate the open circuit impedance matrix of the twin-T, it is useful to first obtain its general equivalent  $\pi$ -network. This can be simply obtained by converting each of the two T-networks of the twin-T into its equivalent  $\pi$ -network. This is shown in Figs. 13a and 13b, assuming sinusoidal input signals. The two resulting  $\pi$ -networks can then be connected in parallel (as shown in Fig. 13c), and the resulting impedance directly calculated. With the two conditions for a perfect null given by equations (5) and (6), we get a simple  $\pi$ -network as shown in Fig. 14. The corresponding impedances are given by

$$Z_a = \frac{R_1}{1 + \frac{\tau_1}{\tau}} \left( 1 + \frac{1}{s\tau} \right), \quad (63)$$

$$Z_b = \frac{R_2}{1 + \frac{\tau_2}{\tau}} \left( 1 + \frac{1}{s\tau} \right), \quad (64)$$

and

$$Z_c = R_s \frac{\left( 1 + \frac{1}{s\tau} \right)}{s\tau_s + \frac{1}{s\tau}}, \quad (65)$$

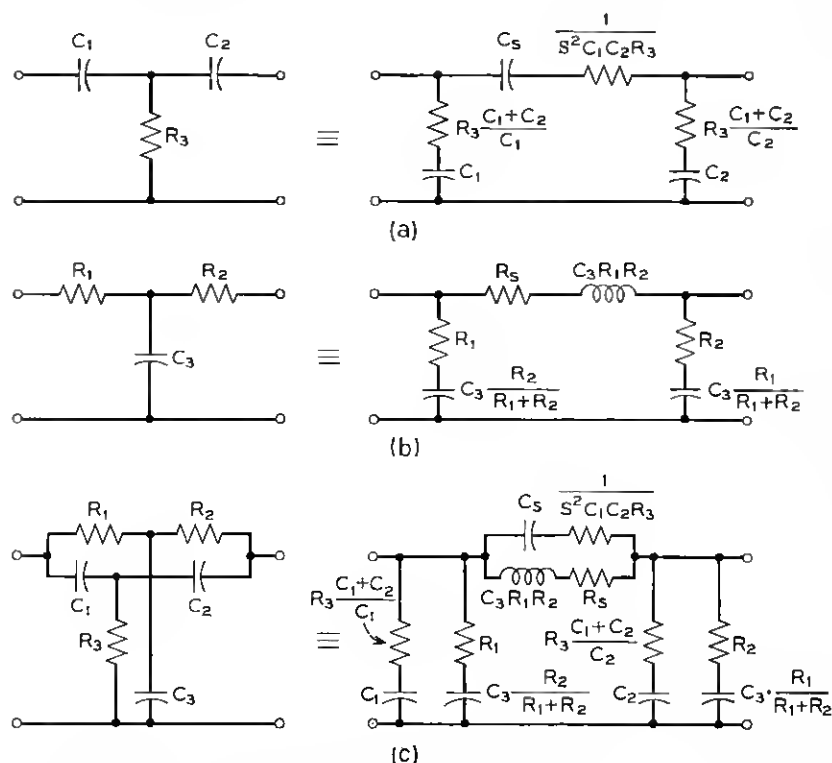


Fig. 13—(a) and (b), Conversion of the two T-networks of the twin-T into equivalent  $\pi$ -networks; (c), Equivalent  $\pi$ -network of the twin-T.

where

$$\tau_1 = R_1 C_1,$$

$$\tau_2 = R_2 C_2,$$

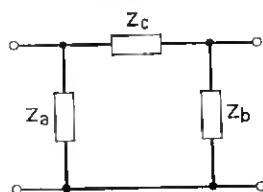
$$\tau_s = R_s C_s,$$

$$\tau = R_p C_3 = R_s C_p.$$

In terms of these impedances, the open-circuit impedance matrix for the twin-T simply follows as

$$[z] = \frac{1}{Z_a + Z_b + Z_c} \begin{bmatrix} Z_a(Z_b + Z_c) & Z_a Z_b \\ Z_a Z_b & Z_b(Z_a + Z_c) \end{bmatrix}. \quad (66)$$

So far we have considered a general twin-T that has an infinite null

Fig. 14—General  $\pi$ -network.

at a specified frequency  $\omega_N$ . Because the corresponding general transfer function [see equation (10)] has the form of a quadratic fraction, it has geometric symmetry around  $\omega_N$ .

The most frequently used twin-T is structurally (and electrically) symmetrical. For this case.

$$\tau_1 = \tau_2 = \tau_s = \tau = RC, \quad (67)$$

$$R_3 = R/2, \quad (68)$$

and

$$C_3 = 2C. \quad (69)$$

The impedances of Fig. 14 then become

$$Z_a = Z_b = \frac{R}{2} \left( 1 + \frac{1}{s\tau} \right) \quad (70)$$

and

$$Z_c = 2R \frac{(1 + s\tau)}{1 + s^2\tau^2}. \quad (71)$$

The open-circuit impedance matrix consequently becomes

$$(z)_o = \frac{R}{4} \begin{bmatrix} \frac{1 + 4s\tau + s^2\tau^2}{s\tau(1 + s\tau)} & \frac{1 + s^2\tau^2}{s\tau(1 + s\tau)} \\ \frac{1 + s^2\tau^2}{s\tau(1 + s\tau)} & \frac{1 + 4s\tau + s^2\tau^2}{s\tau(1 + s\tau)} \end{bmatrix}. \quad (72)$$

The voltage transfer function for the symmetrical twin-T then follows as

$$T_{N_1}(s) = \frac{z_{21o}}{z_{11o}} = \frac{s^2\tau^2 + 1}{s^2\tau^2 + 4s\tau + 1}. \quad (73)$$

Comparing with the transfer function given by equation (10), we have

$$\omega_{N_s} = \frac{1}{RC}, \quad (74)$$

$$2\sigma_{N_s} = \frac{4}{RC} \quad (75)$$

and the inverse damping factor

$$q_{N_s} = 0.25. \quad (76)$$

It can be shown that the selectivity, that is, the inverse damping factor, can be increased by modifying the symmetrical twin-T into a potentially symmetrical network. This is possible with any structurally symmetrical network for which Bartlett's bisection theorem holds. A symmetrical network can be converted into a potentially symmetrical network by impedance scaling one half of the network by some factor  $\rho$ . This is shown for the twin-T in Fig. 15. The corresponding  $z$ -matrix then becomes:

$$(z)_{ps} = \frac{\rho}{1 + \rho} \cdot \frac{R}{2} \begin{bmatrix} \frac{s^2\tau^2 + 2\left(1 + \frac{1}{\rho}\right)s\tau + 1}{s\tau(1 + s\tau)} & \frac{1 + s^2\tau^2}{s\tau(1 + s\tau)} \\ \frac{1 + s^2\tau^2}{s\tau(1 + s\tau)} & \frac{s^2\tau^2 + 2(1 + \rho)s\tau + 1}{s\tau(1 + s\tau)} \end{bmatrix} \quad (77)$$

and the voltage transfer function results as

$$T_{N_{ps}} = \frac{z_{21ps}}{z_{11ps}} = \frac{s^2\tau^2 + 1}{s^2\tau^2 + 2\left(1 + \frac{1}{\rho}\right)s\tau + 1}. \quad (78)$$

In terms of the transfer function (10) we find:

$$\omega_{N_{ps}} = \frac{1}{RC}, \quad (79)$$

$$2\sigma_{N_{ps}} = \frac{2}{RC} \left( \frac{\rho + 1}{\rho} \right) \quad (80)$$

and

$$q_{N_{ps}} = \frac{1}{2} \frac{\rho}{1 + \rho}. \quad (81)$$

$\rho$  gives a measure of the twin-T symmetry. For the extreme asymmetrical



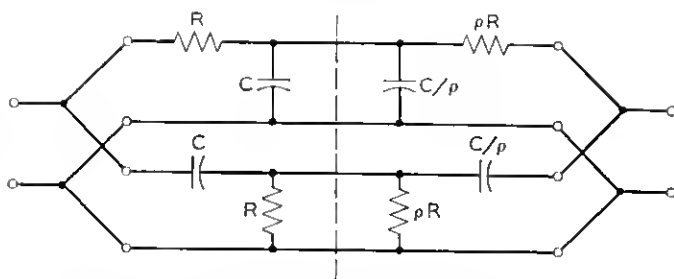


Fig. 15—Potentially symmetrical twin-T resulting from symmetrical twin-T after one-half of the twin-T has been impedance-scaled by a factor  $\rho$ .

case for which  $\rho \gg 1$ ,  $q_{N_p}$ , takes on its maximum value, namely

$$q_{N_p} \big|_{\rho \rightarrow \infty} \rightarrow \frac{1}{2}. \quad (82)$$

## APPENDIX B

### *Twin-T with a Finite Null*

Inspection of equations (8) and (9) shows that the transfer function of a general twin-T is simplified by one degree due to the pole-zero cancellation on the negative real axis at  $\omega_1 = 1/R_3 C_p$  when the conditions for a perfect null given by equations (5) and (6) are satisfied. We investigate here the conditions necessary to ensure this pole-zero cancellation when the null-conditions are only approximately satisfied, that is, when the twin-T has a finite null. To do so we derive the sensitivity of the pole and zero at  $\omega_1$  with respect to the six parameters of the twin-T and investigate under which conditions the respective pole and zero sensitivities are the same.

Writing the twin-T transfer function in the bilinear form with respect to a parameter  $x$  we obtain:

$$T_N(s) = \frac{N(s)}{D(s)} = \frac{A_x(s) + xB_x(s)}{U_x(s) + xV_x(s)}. \quad (83)$$

The sensitivity of a zero  $z$  with respect to  $x$  is then given by:

$$S_z^x = \frac{(s-z)A_x(s)}{N(s)} \bigg|_{s=z} = -x \frac{(s-z)B_x(s)}{N(s)} \bigg|_{s=z} \quad (84)$$

that of a pole  $p$  with respect to  $x$  by

$$S_p^x = \frac{(s-p)U_x(s)}{D(s)} \bigg|_{s=p} = -x \frac{(s-p)V_x(s)}{D(s)} \bigg|_{s=p}. \quad (85)$$

From equations (84) and (85) we obtain

$$S_z^*|_{s=-\omega_1} = \frac{\omega_1}{1 + \alpha^2} \cdot A_z(-\omega_1) \quad (86)$$

and

$$S_z^*|_{s=-\omega_1} = \frac{\omega_1}{1 + \alpha^2 - \frac{\alpha}{q_N}} \cdot U_z(-\omega_1) + \frac{\omega_1}{\left(1 - \frac{1}{1-\lambda}\right) + \alpha^2 \left(1 - \frac{1}{1-\nu}\right)} U_z(-\omega_1) \quad (87)$$

where

$$\alpha = \frac{\omega_1}{\omega_N}, \quad (88)$$

$$\lambda = \frac{R_1}{R_1 + R_2}, \quad (89)$$

$$\nu = \frac{C_1}{C_1 + C_2}, \quad (90)$$

and

$$q_N = \frac{\omega_N}{2\sigma_N} = \frac{\alpha(1-\nu)(1-\lambda)}{\alpha^2(1-\lambda) + (1-\nu)}. \quad (91)$$

Calculating the respective  $A_z(-\omega_1)$  and  $U_z(-\omega_1)$  functions we obtain the zero and pole sensitivities listed in Table IV. Comparing the functions listed in the two columns of the table it is clear from inspection that they will be equal when

$$\frac{\lambda(1-\nu)}{\nu(1-\lambda)} = 1. \quad (92)$$

With equations (88) through (90), this condition becomes

$$R_1 C_1 = R_2 C_2. \quad (93)$$

Thus for all twin-T configurations in which the time constants of the series elements are the same, pole-zero cancellation on the negative real axis is maintained for differentially small perturbations of any element of the twin-T. For positive element changes (that is, increasing values) the dipole frequency will decrease, that is, move in the direction of the origin of the  $s$ -plane. Twin-T networks that satisfy equation (93)

TABLE IV—SENSITIVITY FUNCTIONS FOR THE NEGATIVE REAL POLE AND ZERO OF THE TWIN-T LOCATED AT  $-\omega_1$ 

Zero Sensitivity	Pole Sensitivity
$S_{R_1}^{-\omega_1} = \omega_1 \frac{\alpha^2}{1 + \alpha^2} (1 - \lambda)$	$S_{R_1}^{-\omega_1} = \omega_1 \frac{\alpha^2}{\frac{\lambda(1 - \nu)}{\nu(1 - \lambda)} + \alpha^2} (1 - \lambda)$
$S_{R_2}^{-\omega_1} = \omega_1 \frac{\alpha^2}{1 + \alpha^2} \lambda$	$S_{R_2}^{-\omega_1} = \omega_1 \frac{\alpha^2}{\frac{\lambda(1 - \nu)}{\nu(1 - \lambda)} + \alpha^2} \lambda$
$S_{R_3}^{-\omega_1} = \omega_1 \frac{1}{1 + \alpha^2}$	$S_{R_3}^{-\omega_1} = \omega_1 \frac{1}{1 + \alpha^2 \frac{\nu(1 - \lambda)}{\lambda(1 - \nu)}}$
$S_{C_1}^{-\omega_1} = \omega_1 \frac{1 - \nu}{1 + \alpha^2}$	$S_{C_1}^{-\omega_1} = \omega_1 \frac{(1 - \nu)}{1 + \alpha^2 \frac{\nu(1 - \lambda)}{\lambda(1 - \nu)}}$
$S_{C_2}^{-\omega_1} = \omega_1 \frac{\nu}{1 + \alpha^2}$	$S_{C_2}^{-\omega_1} = \omega_1 \frac{\nu}{1 + \alpha^2 \frac{\nu(1 - \lambda)}{\lambda(1 - \nu)}}$
$S_{C_3}^{-\omega_1} = \omega_1 \frac{\alpha^2}{1 + \alpha^2}$	$S_{C_3}^{-\omega_1} = \omega_1 \frac{\alpha^2}{\frac{\lambda(1 - \nu)}{\nu(1 - \lambda)} + \alpha^2}$

include all symmetrical configurations in which the series elements are identical as well as potentially symmetrical configurations in which the series elements are characterized by relations of the type

$$\begin{aligned} R_2 &= aR_1, \\ C_2 &= C_1/a. \end{aligned} \tag{94}$$

#### APPENDIX C

##### *Twin-T Zero Sensitivity*

Expressing the numerator  $N(s)$  of the twin-T transfer function

$$N(s) = A_x(s) + xB_x(s) \tag{95}$$

the null return difference  $F_x^0(s)$  with respect to  $x$  is given by

$$F_x^0(s) = \frac{N(s)}{A_x(s)} = 1 + x \frac{B_x(s)}{A_x(s)}. \quad (96)$$

With equations (1) and (2), the null return difference of the twin-T with respect to its six components can be calculated directly.

To obtain the null return difference of the nulled twin-T, equation (8) can be substituted into equation (96), namely

$$F_x^0(s) = \frac{(s + \omega_1)(s^2 + \omega_N^2)}{\omega_1 \omega_N^2 A_x(s)} \quad (97)$$

where,  $\omega_1 = 1/R_3 C_p = 1/R_p C_3$ . The corresponding zero sensitivity then results as

$$S_x^{j\omega_N} = \frac{s - j\omega_N}{F_x^0(s)} \bigg|_{s=j\omega_N} = \frac{(s - j\omega_N)\omega_1 \omega_N^2 A_x(s)}{(s + \omega_1)(s^2 + \omega_N^2)} \bigg|_{s=j\omega_N} \quad (98)$$

which simplifies to

$$S_x^{j\omega_N} = -\frac{\alpha(1 + j\alpha)}{2(1 + \alpha^2)} \omega_N \cdot A_x(j\omega_N) \quad (99)$$

where  $\alpha = \omega_1/\omega_N$ . The individual  $A_x(j\omega_N)$  functions follow directly from equations (1) and (2). Substituting these into equation (99), the zero sensitivity of the nulled twin-T with respect to its six components is obtained. These are listed in Table I.

#### REFERENCES

1. Augustadt, H. W., Electric Filter, U. S. Patent No. 2, 106, 785, February 1, 1938; see also: "Circuit Classics Electric Filter," Elec. Equipment Eng., No. 33 (February 1965), p. 35.
2. Scott, H. H., "A New Type of Selective Circuit and Some Applications," Proc. IRE, 26, No. 2 (February 1938), pp. 226-235.
3. Tuttle, W. N., "Bridged-T and Parallel-T Null Circuits for Measurements at Radio Frequencies," Proc. IRE, 28, No. 1 (January 1940), pp. 23-30.
4. Hastings, A. E., "Analysis of a Resistance-Capacitance Parallel-T Network and Applications," Proc. IRE, 34, No. 3 (March 1946), pp. 126-129.
5. Stanton, L., "Theory and Application of Parallel-T Resistance Capacitance Frequency-Selective Networks," Proc. IRE, 34, No. 7 (July 1946), pp. 447-456.
6. Wolf, A., "Note on a Parallel-T Resistance-Capacitance Network," Proc. IRE, 34, No. 9 (September 1946), p. 659.
7. Cowles, L. G., "The Parallel-T Resistance-Capacitance Network," Proc. IRE, 40, No. 12 (December 1952), pp. 1712-1717.
8. Oono, Y., "Design of Parallel-T Resistance-Capacitance Networks," Proc. IRE, 43, No. 9 (May 1955), pp. 617-619.
9. Smith, D. H., "The Characteristics of Parallel-T RC Networks," Electronic Engineering, 29, No. 348 (February 1957), pp. 71-77.
10. Bolle, A. P., "Theory of Twin-T RC Networks and their Application to Oscillators," J. British IRE, 13, No. 12 (December 1953), pp. 571-587.
11. Dutta Roy, S. C., "On the Design of Parallel-T Resistance-Capacitance Networks for Maximum Selectivity," J. Inst. Telecommunication Engineers (India), 8, No. 5 (September 1962), pp. 218-223.

12. Mehta, V. B., "Comparison of RC Networks for Frequency Stability in Oscillators," *Proc. IEE*, *112*, No. 2 (February, 1965), pp. 296-300.
13. Slaughter, J. B., and Rosenstein, A. B., "Twin-T Compensation Using Root Locus Methods," *AIEE Trans.*, *81*, Part II, No. 64 (January 1963), pp. 339-350.
14. Lazear, T. J. and Rosenstein, A. B., "Pole-Zero Synthesis and the General Twin-T," *AIEE Trans.*, *83*, Part II, No. 11 (November 1964), pp. 389-393.
15. Barker, A. C. and Rosenstein, A. B., "S-Plane Synthesis of the Symmetrical Twin-T Network," *AIEE Trans.*, Part II, *83*, No. 11 (November 1964), pp. 382-388.
16. Hollister, F. H., and Thaler, C. J., "Symmetrical Parallel-Tee Network—Parameter Plane Analysis and Synthesis," *Proc. Nat. Elec. Conf.*, *21* (October 1965), pp. 430-438.
17. Hollister, F. H., and Thaler, C. S., "Loaded and Null Adjusted Symmetrical Parallel-Tee Network," *Proc. Nat. Elec. Conf.*, *21* (October 1965), pp. 753-758.
18. Mitra, S. K., "A Note on the Design of RC Notch Networks with Maximum Gain," *Proc. IEEE*, *54*, No. 10 (October 1966), p. 1487.
19. Shenoi, B. A., "A New Technique for Twin-T RC Network Synthesis," *IEEE Trans. Circuit Theory*, *CT-11*, No. 3 (September 1964), pp. 435-436.
20. Hakimi, S. L., and Seshu, S., "Realization of Complex Zeros of Transmission by Means of RC Networks," *Proc. Nat. Elec. Conf.*, *13* (October 1957), pp. 1013-1025.
21. Holt, A. C. J., and Reineck, K. M., "Synthesis of RC Zero Sections," *Radio and Electronic Engineer*, *33*, No. 1 (January 1967), pp. 9-15.
22. Hillan, A. B., "The Parallel-T Bridge Amplifier," *J. Inst. Elec. Eng.*, *94*, Part III, No. 27 (January 1947), pp. 42-51.
23. Sallen, R. P., and Key, E. L., "A Practical Method of Designing RC Active Filters," *IRE Trans. Circuit Theory*, *CT-2*, No. 1 (March 1955), pp. 74-85.
24. Bachmann, A. E., "Transistor Active Filters Using Twin-T Rejection Networks," *Proc. IEEE*, *106*, Part B, No. 26 (March 1959), pp. 170-174.
25. Balabanian, N., and Cinkille, I., "Expansion of an Active Synthesis Technique," *IEEE Trans. Circuit Theory*, *CT-10*, No. 2 (June 1963), pp. 290-298.
26. Balabanian, N., and Patel, B., "Active Realization of Complex Zeros," *IEEE Trans. Circuit Theory*, *CT-10*, No. 2 (June 1963), pp. 299-300.
27. Piercey, R. N. G., "Synthesis of Active RC Filter Networks," *ATE J.*, *21*, No. 2 (April 1965), pp. 61-75.
28. Kerwin, W. J., and Huelsman, L. P., "The Design of High Performance Active RC Bandpass Filters," *IEEE Int. Conv. Record*, *14*, Part 10 (March 1966), pp. 74-80.
29. Moschytz, G. S., "Active RC Filter Building Blocks Using Frequency Emphasizing Networks," *IEEE J. Solid-State Circuits*, *SC-2*, No. 2 (June 1967), pp. 59-62.
30. Moschytz, G. S., "Sallen and Key Filter Networks with Amplifier Gain Larger than or Equal to Unity," *IEEE J. Solid-State Circuits*, *SC-2*, No. 3 (September 1967), pp. 114-116.
31. Moschytz, G. S., "Miniaturized Filter Building Blocks Using Frequency Emphasizing Networks," *Proc. Nat. Elec. Conf.*, *23*, (October 1967), pp. 364-369, 1967; also "FEN Filter Design Using Hybrid Integrated Building Blocks," *Proc. IEEE*, *58*, No. 4 (April 1970), pp. 550-566.
32. Moschytz, G. S., "Two-Step Precision Tuning of a Twin-T Notch Filter," *Proc. IEEE*, *54*, No. 5 (May 1966), pp. 811-812.
33. Mitra, S. K., *Analysis and Synthesis of Linear Active Networks*, New York: John Wiley and Sons, Inc., 1969, pp. 172, 202.
34. Hakimi, S. L., and Cruz, J. B., "On Minimal Realization of RC Two-Ports," *Proc. Nat. Elec. Conf.*, *16* (October 1960), pp. 258-267.
35. Parisi, C., "Control of Temperature Coefficient of Resistance by Reactive Sputtering of Tantalum with Nitrogen and Oxygen Simultaneously," *Proc. Elec. Components Conf.*, 1969. Washington, D. C., April 1969, pp. 366-371.

